

## Automated alignment deviation measurement for precast concrete assembly using point cloud-image fusion

Lizhi Long<sup>a</sup>, Wenyao Liu<sup>a</sup>, Shaopeng Xu<sup>a</sup>, Peng Shi<sup>a</sup>, Cheng Zhang<sup>a</sup>, Lu Deng<sup>a,b,c,\*</sup>

<sup>a</sup> College of Civil Engineering, Hunan University, Changsha, China

<sup>b</sup> Key Laboratory of Damage Diagnosis for Engineering Structures of Hunan Province, Hunan University, Changsha, China

<sup>c</sup> State Key Laboratory of Bridge Safety and Resilience, Hunan University, Changsha, China

### ARTICLE INFO

#### Keywords:

Intelligent construction  
Prefabricated concrete structure  
Alignment deviation measurement  
Computer vision  
3D point cloud processing

### ABSTRACT

Current Precast concrete (PC) column assembly methods face difficulties in precisely measuring the deviation between rebars and sleeves. This paper proposes an automated assembly alignment deviation measurement (AADM) method that integrates 3D point cloud data with 2D images through complementary algorithms. The proposed method comprises a Virtual Trial Assembly (VTA) module that extract sleeve and rebar assembly points and an Alignment Deviation Measurement (ADM) module that calculate rebar-sleeve deviation using three non-collinear points extracted from VTA module. Deviation measurement experiments were conducted on both a PC column model and a real component. Results show that the proposed AADM method outperforms the investigated benchmark methods, with extraction errors lower than 1 mm and positioning accuracy within 3 mm, both meeting the specification requirements. These findings indicate the proposed method enables precise deviation measurement before and during hoisting, providing assistance for automated alignment of precast concrete columns.

### 1. Introduction

Precast concrete (PC) structures are increasingly adopted in modern construction owing to their potential to improve construction efficiency, reduce labor costs, and ensure construction quality. Different to cast-in-place construction, PC structure components are produced in factory and connected onsite. As illustrated in Fig. 1, vertical PC components such as columns are usually assembled using grouting sleeve connections. This connection method requires extremely high alignment accuracy between rebars and sleeves, typically with a maximum allowable deviation of 3 mm between their centerlines [1]. Exceeding this tolerance can degrade structural performance and trigger costly rework, offsetting the advantages of prefabrication.

In actual assembly sites, accurate alignment of PC columns relies on two factors [2]: (1) the precise positioning of rebar and sleeves before hoisting (Fig. 1(b)), and (2) the accurate alignment during hoisting (Fig. 1(c)). Before hoisting, workers typically measure rebar spacing manually using a tape measure (Fig. 1(b1)) and adjust positions with a hand hoist. However, even if individual positioning errors of rebar or sleeve satisfy the deviation tolerance, their cumulative deviations can exceed 3 mm limit and impede insertion. Alternatively, workers may

also employ a mechanical aid such as the fixture plate before hoisting (see Fig. 1(b2)). The fixture plate is sized matching the cross-section of the sleeves, to ensure rebars can be properly inserted into the sleeves [3]. If any rebar is misaligned, the fixture plate can assist workers in correcting its position, thereby preventing repeated manual adjustments due to cumulative errors. While it helps correct misalignments and reduces cumulative errors, this method does not quantify alignment deviations, requiring additional manual measurements for fine deviation management [4]. During hoisting, horizontal positioning of PC columns primarily relies on visual estimation (Fig. 1(c)), necessitating repeated lifting and lowering for precise insertion. These manual measurements and mechanical aids are often insufficient to ensure high-precision assembly in practice.

With the development of intelligent construction technologies, researchers have explored using laser, cameras, and computer vision (CV) algorithms to assist the PC components assembly process. Applying these technologies provides quantitative data of PC columns, making it possible to conduct assemblability evaluation before hoisting and simultaneously deviation measurement during the hoisting process. Over the past decades, many researches have been conducted regarding assemblability evaluation and simultaneously monitoring to improve

\* Corresponding author at: College of Civil Engineering, Hunan University, Changsha 410082, China.

E-mail address: [dengl@hnu.edu.cn](mailto:dengl@hnu.edu.cn) (L. Deng).

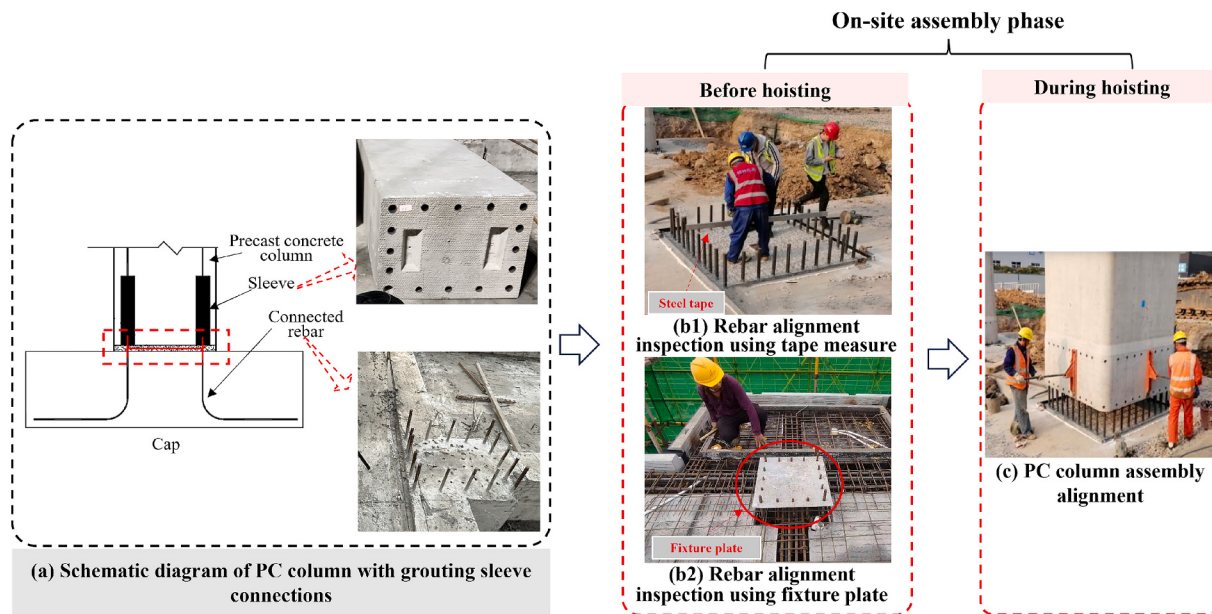


Fig. 1. Schematic diagram assembly of PC column connected by grouting sleeve. Virtual trial assembly (VTA) module

the efficiency and accuracy in PC components alignment process.

(1) **Pre-hoisting assemblability evaluation:** Early research focused on non-contact dimensional inspection methods [5]. Computer vision techniques were applied to assess rebar dimensions before pouring [6,7], overall component dimensions [8–10], and connector positioning after pouring [11,12]. While significant progress has been made in assessing individual component quality, the assessment of assemblability between components remains limited. Later on, Virtual Trial Assembly (VTA) has emerged as an efficient method for assessing component assemblability [13–15]. The VTA technique simulates assembly processes based on Geometric Quality Inspection (GQI) data and quantifying cumulative fabrication errors between assembly components [16]. A critical step in VTA is accurately extracting assembly points from as-built components, as these assembly points directly impact the reliability of pre-assembly evaluation.

Corner points are commonly selected as key assembly features for both GQI and VTA. Due to the large size and surface noise of PC components, existing methods struggle to extract corner features with sufficient accuracy. Kim et al. developed a corner-based feature extraction method for dimensional quality evaluation of PC panels, achieving a measurement accuracy within a 6 mm tolerance [17]. Subsequent research enhanced the corner and edge detection accuracy to 3 mm [18]. These researches concentrated on corner points extraction and neglected the assembly deviation evaluation. Recently, Jiang et al. proposed a VTA method for PC columns based on corner points and simulated dimensional deviations measurement in building information modeling (BIM) models [4]. However, the corners of large PC components, particularly PC columns, are highly prone to damage or loss during transportation and on-site handling, making the corners unreliable as features extraction object. As such, VTA relying on extracting concrete corner points for PC columns assemblability evaluation is often infeasible in practice.

In contrast, the rebars and sleeves at the base of PC columns have obvious features, easier to extract with high accuracy, and less susceptible to damage during construction [6,11]. These features make them ideal as features extraction objects for robust assembly in VTA applications. Therefore, this study proposes using sleeves and connected rebars instead of traditional concrete corners as the main assembly features for VTA of PC columns. This approach may overcome the limitations of corner feature extraction, improving the accuracy and feasibility of assessing PC column assemblability.

(2) **In-hoisting alignment deviation measurement:** Once the assemblability evaluation before hoisting is conducted, simultaneously deviation measurement during the hoisting process must be achieved to ensure the automated assembly process. Some researchers applied terrestrial laser scanning (TLS) to measure positioning deviation in segmental bridge segments and PC pier hoisting [19–21]. However, laser scanning raises high cost and deployment complexity, limiting its widespread adoption.

Image-based CV techniques provide low-cost alternatives for structural displacement measurement [22–25]. Park et al. developed a multi-camera optical motion capture method for 3D displacement measurement [22]. Choi et al. combined Direct Linear Transformation (DLT) and Monte Carlo Localization (MCL) to address occlusion and blurring issues [23]. Cheng et al. [25] proposed a stereo-vision technique for 6-DoF pose tracking. However, these methods typically require the attachment of artificial markers on component surfaces, complicating field deployment.

Recent studies aim to eliminate the need for artificial markers, enhancing adaptability [2,26]. Zhang et al. proposed a vision-based intelligent alignment system predicting target assembly trajectories without markers. The system does not directly measure alignment deviations, instead the trajectory strategy is given by integrated deep learning algorithms, resulting lower explainability [26]. Ye et al. proposed a method using conventional image processing algorithms to quantify alignment deviations between sleeves and rebars in PC columns [2]. However, the method was validated only on small 3D-printed models and lacks robustness against real PC columns with high noise.

In summary, although significant progress has been made in both pre-hoisting assemblability evaluation and in-hoisting alignment deviation measurement, research gaps still exist when aiming at an automated assembly process. First, current research remains on PC columns VTA often chooses corners as features extraction objects, highly prone to damage or loss during transportation and on-site handling. Second, existing alignment deviation measurement methods based on laser-scanning and image-based CV techniques can not achieve satisfying balance between cost and performance. Furthermore, there is still a lack of an integrated deviation measurement method that spans both stages, particularly designed for the assembly of PC components under stringent tolerance requirements.

To address this gap, this paper proposes an automated method that integrates 3D point cloud and 2D image data to accurately measure

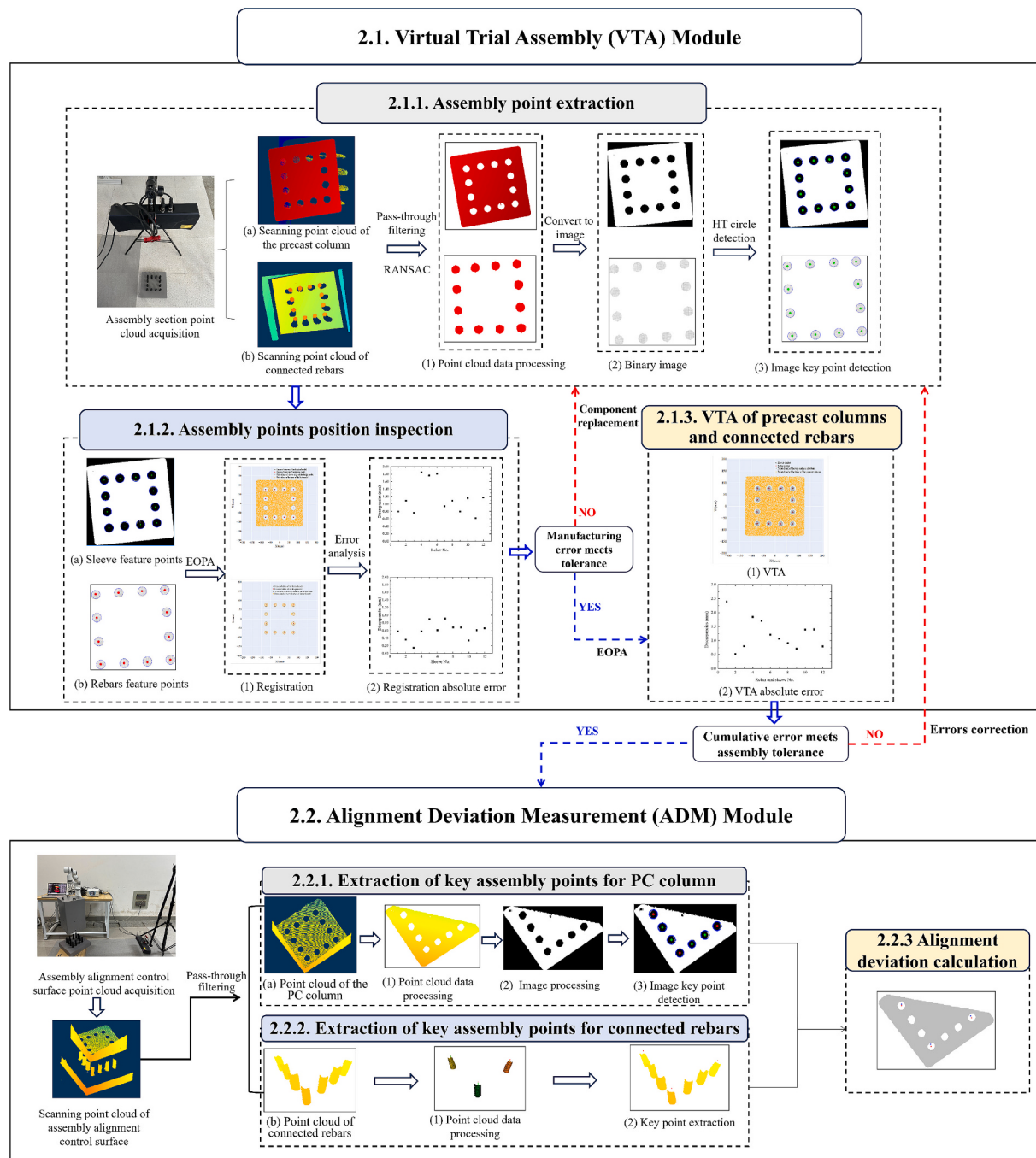


Fig. 2. Research framework.

alignment deviations during the assembly of precast concrete (PC) columns. This method addresses both pre-hoisting assemblability evaluation and in-hoisting positioning measurement, enabling high-precision automated assembly of PC components within strict tolerance constraints (3 mm). It consists of two modules: (1) Virtual Trial Assembly (VTA) Module: This module aims to estimate the assemblability of PC columns before hoisting by automatically measuring pre-assembly alignment deviations. It preprocesses the 3D point clouds of rebars and sleeves, converts them to image format, extracts key assembly points using Hough Transform (HT) circle detection [27], and evaluates pre-assembly errors with the Extended Orthogonal Procrustes Analysis (EOPA) algorithm [13]. (2) Alignment Deviation Measurement (ADM) Module: This module employs a strategy based on three non-collinear assembly feature points to automatically determine the deviation

between the PC column and connected rebars during the hoisting process, facilitating high-precision on-site assembly alignment. The proposed method provides a theoretical and technical foundation for the intelligent hoisting and high-precision assembly of PC columns connected by grouting sleeves.

This paper is organized as follows. Section 2 presents the methodology, which consists of two core modules: a VTA module for pre-hoisting assemblability evaluation and an ADM module for in-hoisting component poistioning. Section 3 reports the laboratory experiments validating the method with 3D-printed precast components. Section 4 describes the field tests on full-scale PC columns to further evaluate the method's on-site applicability and robustness. Finally, Section 5 summarizes the conclusions and suggests directions for future work.

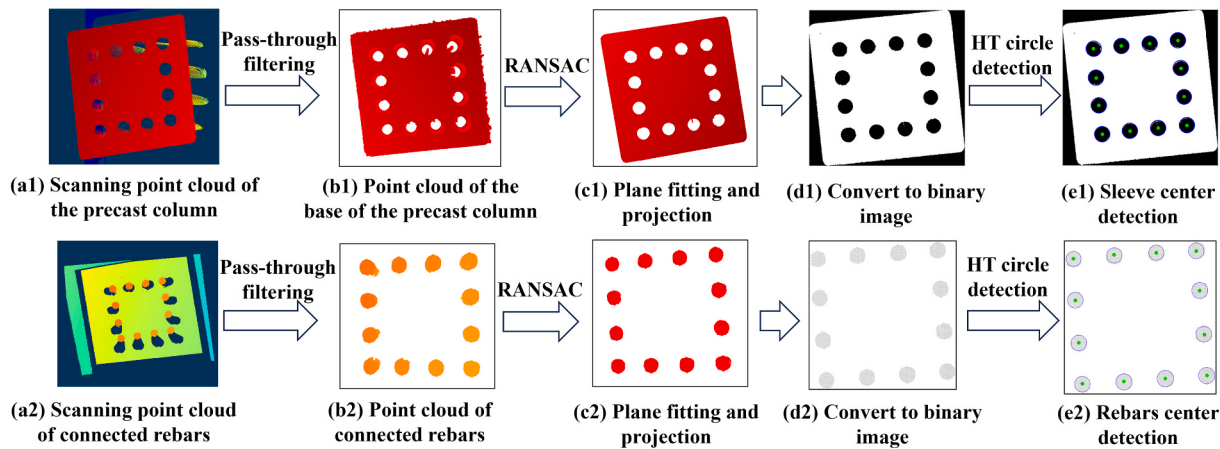


Fig. 3. Assembly points extraction of the precast column and connected rebars of the as-built model.

## 2. Methodology

This study proposes an automated method for measuring assembly alignment deviation in PC components by fusing 3D point clouds and 2D images. It utilizes 3D point clouds obtained from a structured light camera, as shown in Fig. 2, which includes two main modules:

### 2.1. Virtual trial assembly (VTA) module

It employs CV and Extended Orthogonal Procrustes Analysis (EOPA) to assesses the assemblability of PC components [13]. The process involves extracting assembly points of PC column and connected rebars (2.1.1), detecting their positional deviations with EOPA (2.1.2), and performing VTA (2.1.3) if deviations are within fabrication tolerance. The process continues to the second part if the cumulative error is within assembly tolerance.

### 2.2. Alignment deviation measurement (ADM) module

It uses three non-collinear key assembly points, integrating point cloud and image processing techniques to extract key assembly points of PC column (2.2.1) and connected rebars (2.2.2), allowing for the calculation of alignment deviation (2.2.3).

### 2.3. Virtual trial assembly (VTA) module

#### 2.1. Virtual trial assembly (VTA) module

Current methods for measuring rebar positioning measurement are inadequate for ensuring accurate alignment of PC columns before hoisting. To address this limitation, a VTA method is proposed, incorporating CV and Extended Orthogonal Procrustes Analysis (EOPA). The approach includes three key components: (1) extraction of assembly points, (2) inspection of their positions, and (3) VTA of the PC column and connected rebars.

#### 2.1.1. Assembly point extraction

This study examines the grouting sleeve connection of PC columns, identifying the centers of the bottom sleeves and the top surfaces of connected rebars as assembly points. To facilitate VTA, an automatic assembly point extraction algorithm using CV is developed. The process for extracting the assembly points from the as-built point cloud model involves several steps, as illustrated in Fig. 3. Initially, a structured light camera is utilized to vertically capture the scan data (see Fig. 3a) of the bottom sleeves of the precast column and the top of the connected rebars. Subsequently, a pass-through filter along the Z-axis with specified range thresholds is applied to eliminate noise, resulting in point clouds (see Fig. 3b) that represent the bottom of the precast column and the top of the connected rebars. The Random Sample Consensus (RANSAC) [28] algorithm is then employed to fit the planes (see Fig. 3c) to the point clouds corresponding to the precast column bottom and the top of the connected rebars. Specifically, the RANSAC plane fitting seeks the best-fitting plane equation  $ax + by + cz + d = 0$ , where  $(x, y, z)$  are point coordinates, and  $a$ ,  $b$ , and  $c$  are the normal vector components, while offset  $d$  indicates the plane's distance from the origin. An inlier distance threshold of 50 mm is set, meaning a point is an inlier if its perpendicular distance to the fitted plane is less than 50 mm. The method uses 500 iterations to ensure robustness against outliers. Point clouds are projected onto the fitted planes to derive the 2D point cloud planes of the precast column bottom and the rebar top surface, respectively. The orthogonal projection of a point  $p = (x, y, z)$  onto the fitted plane  $ax + by + cz + d = 0$  is computed as:

$$P' = P - \left( \frac{ax + by + cz + d}{a^2 + b^2 + c^2} \right) (a, b, c) \quad (1)$$

where  $p'$  is the projected point on the plane. This operation ensures that the 3D point clouds of sleeves and rebars are accurately flattened onto their planes for 2D image conversion and circle detection.

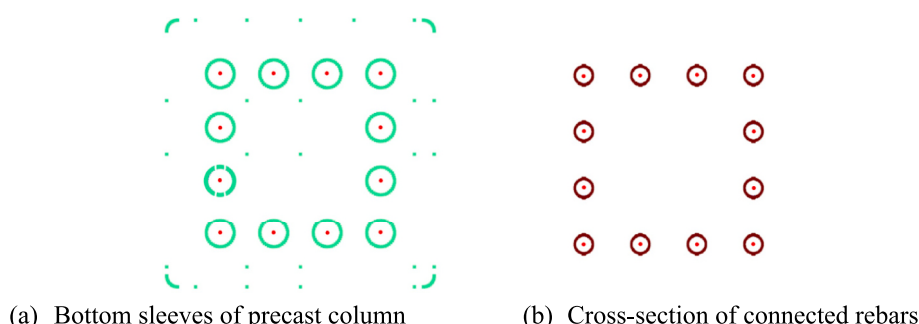


Fig. 4. As assembly point extraction of the precast column and connected rebars of the as-designed model.

Subsequently, the 2D point cloud planes are transformed into binary images through image mapping and normalization (see Fig. 3d). To map the point coordinates to the image pixel coordinate system, the 2D coordinates are first linearly scaled and their bounding ranges are calculated for determining the resolution of the output image. On this basis a grey scale image initially all black is created and the position of each point is marked as a white pixel point, thus forming a binarized image (e.g., the column's bottom surface in Fig. 3(d1)) of point clouds. To differentiate between the sleeve and connected rebar images, black pixel points in the rebar image represent the rebar point cloud, while white pixel points indicate the background (see Fig. 3(d2)). The Hough Transform (HT) Circle detection algorithm [27] is then utilized to extract the centers of the sleeves and the rebars from these images (see Fig. 3e). The minimum and maximum detection radii are based on the actual diameters of the sleeve and rebar. An accumulator threshold of 30 means only circles with at least 30 votes are considered valid for detection, ensuring accurate recognition of circular features despite noise in the binary image.

To extract assembly points from the as-designed model, the 3D as-designed models of the precast column and the connected rebars are first converted into point cloud models in Point Cloud Data (PCD) format. These point cloud models are then filtered using a pass-through filter to isolate the edge point clouds of the precast column's bottom sleeves and the connected rebars' top surface. The average values of the edge point clouds are computed to determine the centers of the sleeves and the top surfaces of the rebars, as shown in Fig. 4.

### 2.1.2. Assembly points position inspection

The mismatch between the dimensions and positions of the sleeves and the connected rebars in PC columns significantly complicates the alignment process during hoisting at construction sites [11]. Since the dimensions of the grouting sleeves and rebars are verified for compliance before leaving the factory, dimensional verification is not within the scope of this work. Instead, it addresses the primary concern of positional mismatch, particularly the misalignment of rebars resulting from collisions that occur during transportation and assembly at the construction site. Such misalignment frequently hinders successful assembly. Consequently, it is imperative for construction workers to verify the positioning of the connected rebars before the hoisting. This verification is especially critical as outlined in the “Standard for tolerances for PC components” (T/CCES 30–2022) [29], Section 4.3.3, which state: “The deviation of the centerline positions of adjacent reserved connected rebars or sleeves should not exceed 2 mm.”

The Extended Orthogonal Procrustes Analysis (EOPA) [13] algorithm is employed to calculate the least-squares deviation between the assembly point positions of sleeves and rebars and their corresponding design positions, thereby assessing the positional accuracy of the assembly points. EOPA, which is an extension of Procrustes Analysis (PA), is a widely recognized mathematical technique applied in various fields, including CV [30], procrustean photogrammetry [31], and shape analysis [32]. This technique is employed to align and compare two sets of point data, such as 3D point clouds or shapes. The method is predicated on the least squares approach, which facilitates the transformation of coordinate matrices to optimize the alignment between the transformed and target matrices. Specifically, given two point sets designated as the target point set  $Y_{c \times k}$  and the point set  $X_{c \times k}$  to be aligned. These sets represent the spatial coordinates of the assembly points of the precast component design model and the completion model, or alternatively, the connected rebar design model and completion model, respectively. Here,  $k = 3$  represents three-dimensional coordinates, and  $c = 12$  represents the 12 alignment feature points. To achieve the matching, the matrix  $X$  must undergo a coordinate transformation to best align with matrix  $Y$ , as shown in Eq. (2).

$$Y = XR + jt^T + E \quad (2)$$

where  $R_{k \times k}$  is a rotation matrix,  $t_{k \times 1}$  is a translation vector,  $j_{k \times 1}$  is an auxiliary unitary vector ( $j^T = (1, 1, \dots, 1)$ ), and  $E$  is an error matrix. The objective is to determine the transformation parameters  $R$  and  $t$  that minimize the square of the 2-norm of  $E$ , that is,

$$\|E\|^2 = \min \left\{ \|XR + jt^T - Y\|^2 \right\} \quad (3)$$

This equation can be solved using the method of Lagrange multipliers. Based on the properties of orthogonal matrices, Singular Value Decomposition (SVD) is applied to solve the problem. For detailed information, please refer to the literature [[14,33]]. The SVD process is as follows:

$$VDW^T = U = X^T \left( I - \frac{jj^T}{P} \right) Y \quad (4)$$

where  $V$ ,  $D$ , and  $W$  are the matrices obtained by SVD of the right matrix  $U$ ,  $I$  is  $R^T R$ , the scalar  $P$  is the number of rows of the matrices  $X$  and  $Y$ , and the coordinate transformation parameters (rotation matrix  $R$  and translation vector  $t$ ) can be obtained using the following formulas:

$$R = VW^T \quad (5)$$

$$t = (Y - XR)^T \frac{j}{P} \quad (6)$$

### 2.1.3. VTA of precast column and connected rebars

Even if the fabrication errors of the precast column's bottom sleeves connected rebars are within the tolerance, they may not connect directly. Significant dimensional errors can lead to a relative fabrication error exceeding allowable limits. According to Section 10.4 of the *Technical Standard for Assembled Buildings with Concrete Structure* (GB/T 51231–2016) [1], the maximum allowable alignment deviation between the center of the connected rebar and the sleeve during field installation is within 3 mm. This 3 mm tolerance specifically applies to the on-site alignment phase, and is distinct from the 2 mm pre-hoisting fabrication tolerance mentioned earlier. Thus, conducting a Virtual Trial Analysis (VTA) on the precast column before assembly is essential to evaluate fabrication and assembly errors. The EOPA algorithm, described in Section 2.1.2, is employed to align the given two sets of points, where the target point set  $Y_{p \times k}$  represents the assembly points of the sleeve in the as-built model of the precast column, and the point set  $X_{p \times k}$  to be aligned represents the assembly points of connected rebars in the as-built model. The subsequent calculations are described in Section 2.1.2. During the VTA process for the precast column, if a collision occurs between the sleeve and the connected rebars, the collision should be resolved by replacing or fine-tuning the components. During the adjustment process, it is essential to ensure that the deviation between the assembly components and their design model complies with the standard requirements.

### 2.2. Alignment deviation measurement (ADM) module

This section presents a method for measuring alignment deviations using three non-collinear key assembly points. By accurately determining these points and calculating the resulting deviation, the alignment of the precast column assembly process can be effectively monitored. Three non-collinear points uniquely define a plane in three-dimensional space, simplifying the assembly alignment problem: if all reserved rebars are inserted into the precast column's bottom sleeves, the goal is to align the center points of the top surfaces of three non-collinear rebars with their corresponding sleeve center points. This simplification is based on the assumption that the bottom plane of the precast column and the connected rebars behave as a rigid body during hoisting. It also assumes that the manufacturing errors of the sleeves and rebars comply with the  $\pm 2$  mm tolerance specified in the T/CCES 30–2022 standard, and that their pre-assembly alignment deviation ( $\pm$

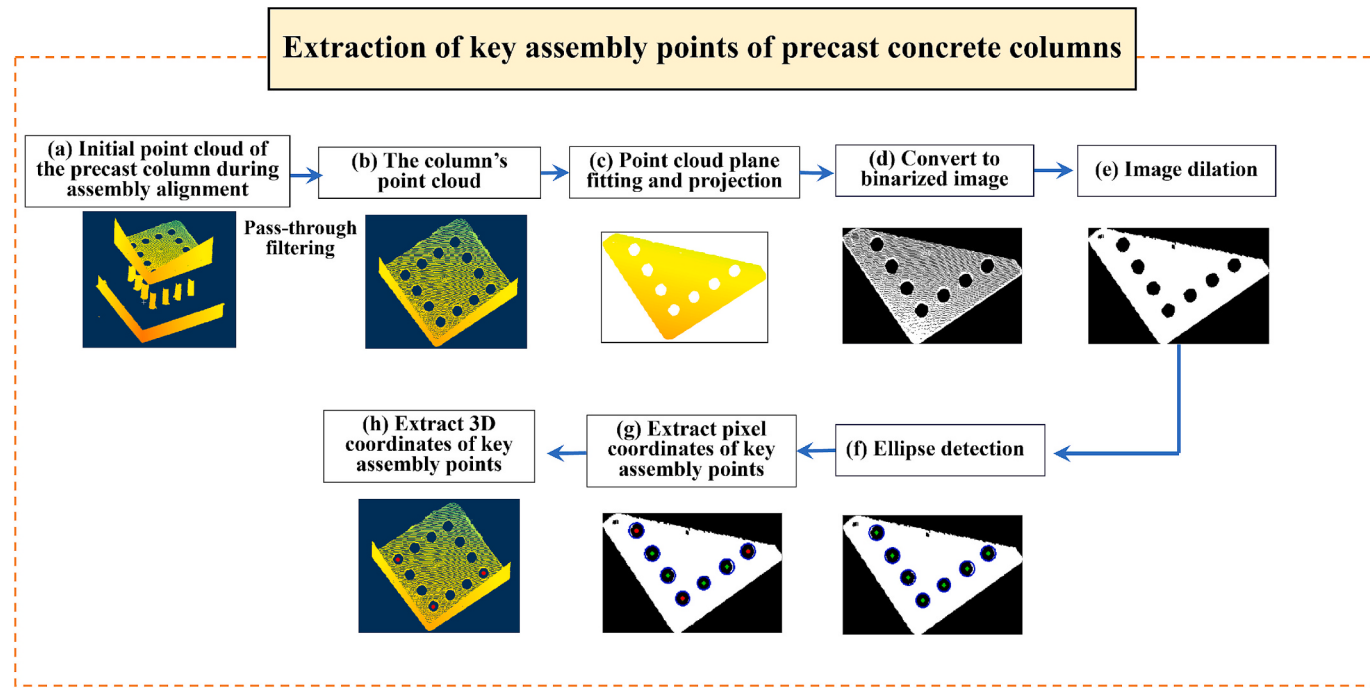


Fig. 5. Flowchart for extracting key assembly points of the precast column.

3 mm) have been verified by the proposed VTA module. Under these conditions, the alignment state of the entire sleeve–rebar interface can be reasonably inferred from the deviation of three key reference points. The method involves three steps: (1) extracting key assembly points from the precast column, (2) extracting key assembly points from the connected rebars, and (3) calculating the assembly alignment deviation of the precast column components.

#### 2.2.1. Extraction of key assembly points for PC column

This section focuses on the precast rectangular column, selecting three center points of the sleeves near the rectangular corners of the bottom surface as the key assembly points for alignment. A method for extracting these points is proposed, with the main steps illustrated in Fig. 5. Initially, a structured light camera was utilized to capture the point cloud of the precast column's assembly control plane as raw data (see Fig. 5a). The assembly control plane is defined as the entire scene of the alignment process viewed along the camera's line of sight. Point clouds of the precast column and the connected rebars are extracted using direct pass-through filtering along the y-axis of the camera's coordinate system. The Random Sample Consensus (RANSAC) algorithm [28] is then applied to the point cloud of the precast column to fit a plane, determining the spatial plane of the bottom surface of the column (see Fig. 5c). The fitted plane is expressed as equation  $ax + by + cz + d = 0$ . The RANSAC fitting uses an inlier distance threshold of 50 mm and 500 iterations to ensure robustness. All point clouds within this plane are then projected onto the fitted plane. The orthogonal projection of a point  $p = (x, y, z)$  onto the plane is computed by eq. (1). The projected point cloud is subsequently converted into a binary image. To translate the point coordinates of the column's bottom surface into the image pixel coordinate system, the 2D coordinates undergo a linear scaling process, followed by the calculation of their bounding ranges to establish the resolution of the resultant image. A grayscale image, initially black, is created, with white pixels representing the column's point cloud, resulting in a binarized image (see Fig. 5d). It is important to note that the structured light camera (Mech-Eye PRO M) employed is suitable for mid-to-long-range imaging, which refers to a best working distance of approximately 1.0 to 2.0 m. However, its fixed resolution of the camera results in sparser point clouds at greater distances. Consequently, the

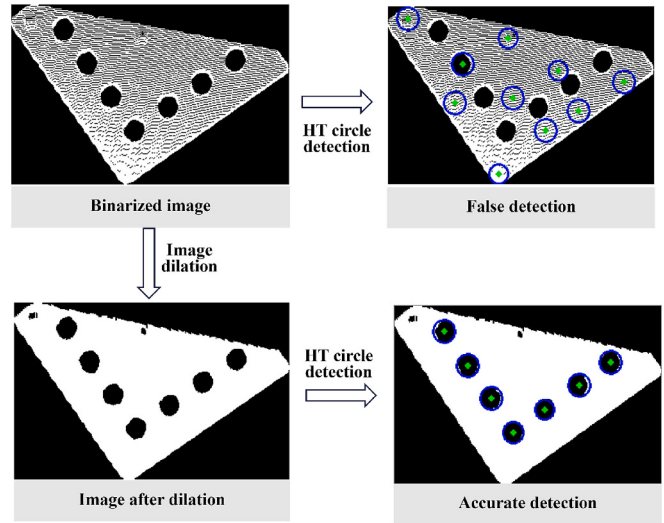
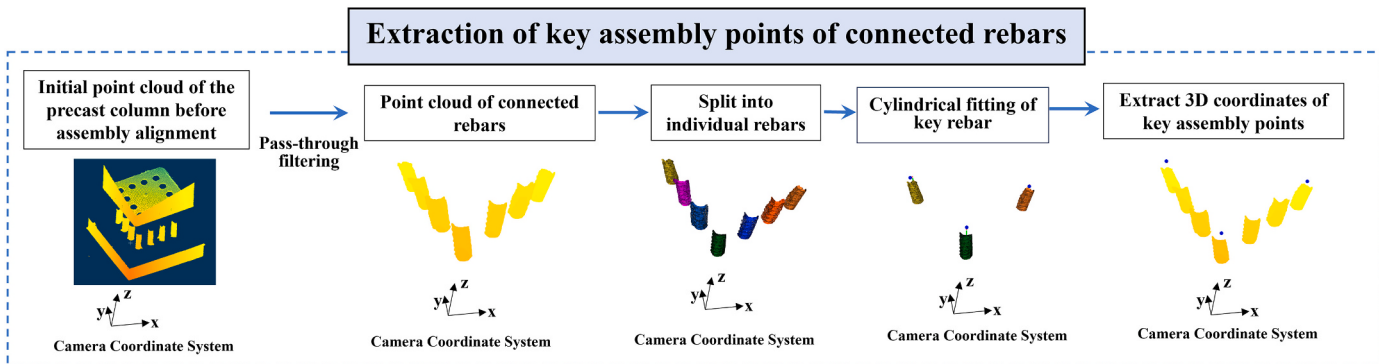


Fig. 6. Morphological dilation operation.

binary image displays sparse black points on the bottom surface of the column, as shown in Fig. 5d. During the subsequent HT circle detection [27], these black points are treated as noise, often leading to circle fitting failures, as shown in Fig. 6. To mitigate this issue, a morphological dilation operation [34] is first applied to the binary image, expanding the white regions and effectively eliminating the black point noise. A morphological dilation using a  $3 \times 3$  kernel expands the boundaries of white regions and suppresses isolated black noise. The processed image then undergoes HT circle detection to extract sleeve centers with the minimum and maximum radii set according to actual sizes. An accumulator threshold of 30 requires a circle to receive at least 30 votes to be valid, resulting in the identification of the radii and image coordinates of the seven sleeve centers at the bottom of the column. Finally, the image coordinates of the seven sleeve center points are converted into three-dimensional coordinates in the camera's coordinate system. The 2D image coordinates ( $u, v$ ) are converted into 3D points ( $X$ ,



**Fig. 7.** Flowchart for extracting key assembly points of the connected rebars.

$Y, Z$ ) by using the known depth  $Z$  (measured during scanning) and the intrinsic parameters of the camera. The conversion follows the pinhole camera model:

$$X = (u - c_x) \frac{Z}{f_x}, Y = (v - c_y) \frac{Z}{f_y} \quad (7)$$

where  $(c_x, c_y)$  are the principal point offsets, and  $(f_x, f_y)$  are the focal lengths in pixel units.

The three key assembly points are selected as the two sleeve centers with the maximum and minimum x-coordinates and the sleeve center with the minimum z-coordinate. Where all coordinates are considered in the camera coordinate system.

### **2.2.2. Extraction of key assembly points for connected rebars**

This section identifies three critical assembly points for connected rebars by locating the centers of their top surfaces, corresponding to the precast column's designated assembly points. The method, as illustrated in Fig. 7, comprises three main steps: rebar segmentation, cylinder fitting, and key point selection.

### **Step 1: Rebar segmentation using DBSCAN.**

The point cloud of the connected rebars is first segmented into individual bars using the Density-Based Spatial Clustering of Applications with Noise (DBSCAN) algorithm [35]. DBSCAN groups points into clusters based on their spatial proximity. The Euclidean distance  $D$  between any two points  $P_i = (x_i, y_i, z_i)$  and  $P_j = (x_j, y_j, z_j)$  is computed as:

$$D = \min \left\| P_i - P_j \right\|_2 \geq d_{th} \quad (8)$$

$$D = \sqrt{(x_i - x_j)^2 + (y_i - y_j)^2 + (z_i - z_j)^2} \quad (9)$$

where the input point cloud  $\{P\}$  is assumed to have  $n$  clusters  $\{C_i|i, i+1, \dots, [1, n]\}$ , assuming that  $C_i = \{P_i \in P\}$  and  $C_j = \{P_j \in P\}$  are different clusters among them, the point in  $\{C_i\}$  is  $P_t$ , the point in  $C_j$  is  $P_j$ ,  $D$  is the distance between points in different clusters, and  $d_{th}$  is the neighbor radius threshold. In this study, each rebar is treated as a

separate cluster, and  $d_{th}$  is set according to the physical distance between the inner edges of two adjacent rebars, ensuring that points from different rebars are not merged into a single cluster.

### **Step 2: Cylinder fitting using RANSAC.**

After segmentation, each rebar cluster is processed using the Random Sample Consensus (RANSAC) algorithm [28] to fit a 3D cylinder model. The resulting cylinder axis is expressed in parametric form as:

$$\mathbf{L}(t) = \mathbf{p}_0 + t \cdot \mathbf{v} \quad (10)$$

where  $p_0$  is a point on the cylinder axis,  $v$  is the axis direction vector, and  $t \in \mathbb{R}$  is a scalar parameter.

The top surface plane of each rebar is estimated through plane fitting, and the intersection point  $P_{top}$  of the cylinder axis with this plane is calculated for each bar. These intersection points represent the approximate centers of the rebar top surfaces.

The intersection coordinates of these centerlines with the plane of the top surface of the rebars are calculated, identifying the maximum and minimum x-coordinates, and the minimum z-coordinate as the key assembly points. The average y-coordinate at top of these rebars is calculated using the 20 points with the largest y-values from each bar's point cloud.

### **Step 3: Selection of key assembly points.**

To compute alignment deviations, three non-collinear key points are selected among the seven  $P_{top}$  candidates. The maximum and minimum x-coordinates, and the minimum z-coordinate are chosen as the key assembly points.

### 2.2.3. Alignment deviation measurement

After obtaining the coordinates of the three key assembly points for the precast column and the three connected rebars, the rebars' coordinates are projected onto the bottom surface of the precast column. The distance between the projected rebars and the column's assembly points is then calculated to determine alignment deviation. The calculation process is illustrated in Fig. 8.

Let the three key assembly points on the precast column be denoted

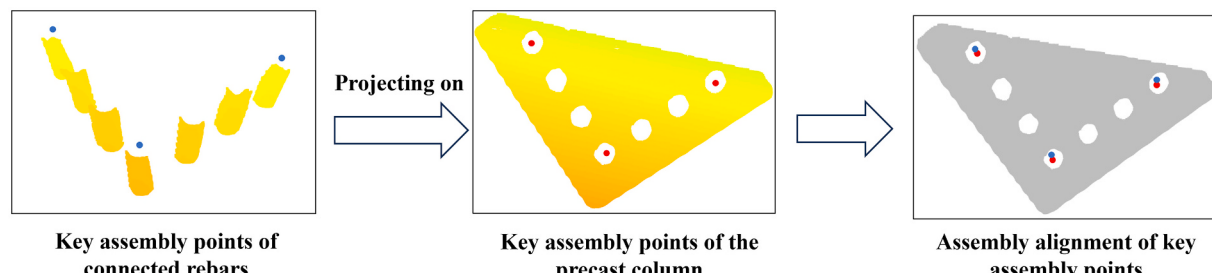


**Fig. 8.** Flowchart for calculating alignment deviation in precast column assembly.

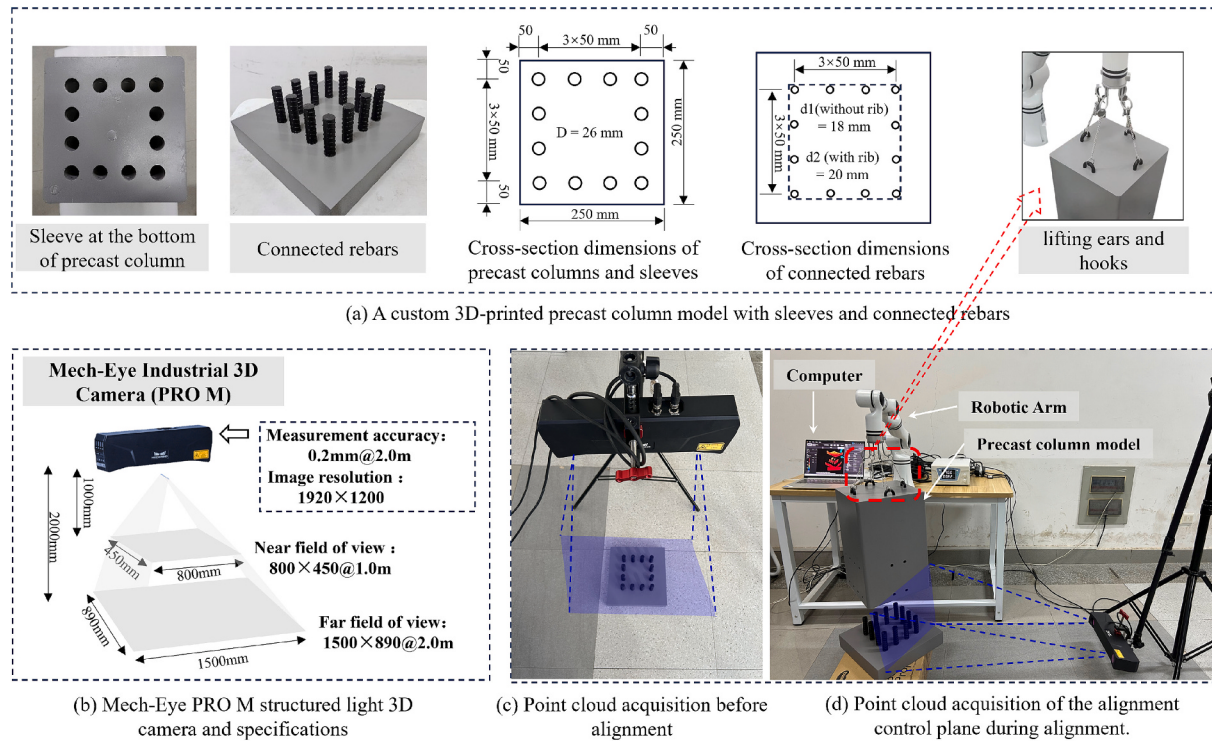


Fig. 9. Point cloud data acquisition system for alignment deviation of precast columns.

as  $P_1^c$ ,  $P_2^c$ ,  $P_3^c$ , and the corresponding key points on the connected rebars as  $P_1^r$ ,  $P_2^r$ ,  $P_3^r$ , where each point  $P = (x, y, z)$  is defined in 3D Cartesian space.

To ensure accurate comparison, each rebar key point  $P_1^r$  is orthogonally projected onto the bottom surface plane of the precast column. This plane is defined based on the column's local coordinate system or fitted from its bottom face point cloud. The projected points are denoted as  $P_i^r$ , where  $i = 1, 2, 3$ .

The alignment deviation for each point pair is computed as the Euclidean distance between the column assembly point and the projected rebar point:

$$d_i = \|P_i^c - P_i^r\|_2 = \sqrt{(x_i^c - x_i^r)^2 + (y_i^c - y_i^r)^2 + (z_i^c - z_i^r)^2}, \quad i = 1, 2, 3 \quad (11)$$

Value  $d_i$  serves as an indicator of the horizontal offset between the rebar set and the precast column, and can be used to guide corrective alignment during the assembly process.

### 3. Laboratory test

To verify the accuracy of the proposed alignment deviation measurement method in practical applications, feasibility testing and parameter analysis were first conducted in a laboratory setting. Given the high-risk and time-sensitive nature of hoisting construction sites, laboratory verification provides necessary data support and optimization for onsite application. 3D-printed models of the precast column and the connected rebars were custom-designed to simulate the actual assembly scenario, and a point cloud data acquisition system was developed for measuring alignment deviation. The experiment was divided into two parts: (1) VTA of the precast column before hoisting and (2) Alignment Deviation Measurement during hoisting process.

#### 3.1. Experimental settings

The point cloud data acquisition system for measuring alignment

deviation in precast columns, developed in a lab, is shown in Fig. 9 and consists of four main components.

- (a) A custom 3D-printed precast column model with sleeves and connected rebars;
- (b) Mech-Eye PRO M structured light 3D camera and specifications;
- (c) Point cloud acquisition before alignment;
- (d) Point cloud acquisition of the alignment control plane during alignment.

The assembly alignment component is shown in Fig. 9 (a). A custom 3D-printed model of a precast column is connected to reserved rebars via the grouting sleeve. Both the precast column and rebar models were fabricated using a high-resolution FDM 3D printer, with a nominal dimensional accuracy of  $\pm 0.1$  mm. Key dimensions were verified using a vernier caliper (0.02 mm resolution), and visibly deformed parts were excluded. Although the printed models do not replicate actual concrete surfaces, they provide a controlled physical reference for validating the measurement method under known geometric conditions. The column base measures 250  $\times$  250 mm, with a sleeve diameter of 26 mm, a rebar diameter (without rib) of 18 mm, and a rebar diameter (with rib) of 20 mm. To ensure successful sleeve–rebar connection, the deviation between the centerlines of the reserved rebar and the sleeve must not exceed 3 mm, as specified in the alignment tolerance standard (GB/T 51231–2016) [1]. The top of the precast column model includes four lifting ears for robotic suspension.

To conduct alignment deviation measurements, a flange with four lifting hooks was fixed to the robotic arm's end effector. The column model is suspended by four equal-length slings for controlled movement.

The structured light camera, shown in Fig. 9 (b), is a Mech-Eye 3D Camera (PRO M) with a resolution of 1920  $\times$  1200 and a measurement accuracy of 0.2 mm at 2 m. Each acquisition produces a grayscale image, a depth map, and a high-precision point cloud. The camera is placed along the diagonal direction of connected rebars to better capture the rebars on both sides of the diagonal, as illustrated in Fig. 9 (c). The measurement is performed in the camera coordinate system.

During alignment, the camera captures the alignment control plane of the precast column, as shown in Fig. 9 (d). The Reirman RM-65B

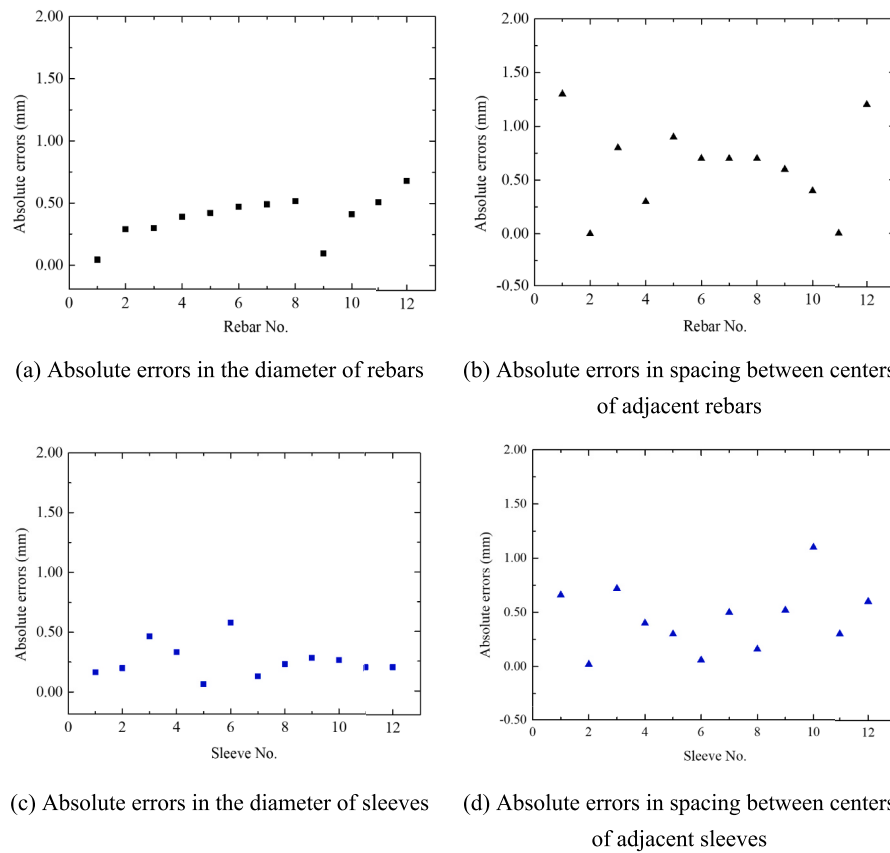


**Fig. 10.** Scatter chart of the accuracy of the assembly point position estimation for the precast column and connected rebars model.

robotic arm has a 5 kg rated payload, a 610 mm working range, and  $\pm 0.05$  mm repeatability accuracy. The host computer, a Lenovo Legion Y7000P, equipped with Windows 11, Intel i7-14650HX CPU, 32 GB RAM, and NVIDIA RTX 4060 (8 GB GPU), with software developed in Python 3.6.

Furthermore, to ensure fairness in our comparative experiment, all methods—including our fusion approach, image-only, and point cloud-only methods—were evaluated using data from a single structured light camera. This device provides synchronized image and point cloud data, ensuring consistent input for all algorithms. This eliminates hardware-related confounding variables, allowing performance comparisons to focus solely on algorithm effectiveness. This unified multi-modal sensor strategy ensures scientific rigor and offers practical cost-efficiency through high integration.

### 3.2. Experimental results of VTA of precast column

This section validates the proposed VTA method for assessing precast column assemblability through laboratory experiments. Section 3.2.1 verifies the assembly point extraction method and its positional accuracy. Section 3.2.2 evaluates the matching accuracy between sleeve and rebar positions to confirm the VTA results' reliability.

**Table 1**

The mean and confidence interval (CI) of the accuracy of the assembly point position estimation for the precast column connected rebars model.

	Mean value (mm)	Standard deviation (mm)	CI (mm)
Rebar diameter	0.38	0.17	(0.29, 0.48)
Adjacent rebar spacing	0.56	0.31	(0.38, 0.74)
Sleeve diameter	0.26	0.14	(0.18, 0.34)
Adjacent sleeve spacing	0.45	0.29	(0.28, 0.61)

#### 3.2.1. Assembly point extraction method validation and assembly point position checking

This subsection verifies the accuracy and reliability of the proposed method for extracting assembly points on the bottom of precast columns and the top of connected rebars. Validation involves two steps: (1) assessing the extraction method's accuracy, and (2) measuring positional deviations between extracted sleeve or rebar assembly points to evaluate alignment consistency.

##### (1) Assembly point extraction method validation.

The extraction of assembly points directly affects the accuracy of the assembly point position estimation and VTA reliability. To assess the accuracy of the proposed method, the diameter and spacing between centers of the adjacent sleeves or the rebars, estimated through the assembly point extraction, were compared to manual measurements taken with a vernier caliper (resolution: 0.02 mm). The uncertainty of these measurements was assessed through three repetitions for each target dimension yielding a standard deviation within 0.05 mm, indicating acceptable reliability as ground truth. The precast column model has 12 sleeves and 12 corresponding rebars, resulting in 24 distances ( $12 \times 2$ ) between adjacent rebars and sleeves, as well as 24 diameters of the rebars and the sleeves, were calculated and compared. Fig. 10 (a), (b), (c), and (d) display the absolute errors between the manually measured and estimated values for the diameter of the connected rebars, the spacing between centers of adjacent rebars, the diameter of the sleeves, and the spacing between centers of adjacent sleeves. Specifically, Fig. 10 (a) shows a mean absolute error of 0.38 mm and the root mean square error (RMSE) of 0.42 mm; Fig. 10 (b) shows a mean absolute error of 0.56 mm and RMSE of 0.64 mm; Fig. 10 (c) shows a mean absolute error of 0.29 mm and RMSE of 0.26 mm; Fig. 10 (d) shows a mean absolute error of 0.45 mm and RMSE of 0.53 mm. Overall, the average absolute error and RMSE for calculated center distances were below the 2 mm tolerance for sleeve and rebar dimensions, confirming the method's accuracy in

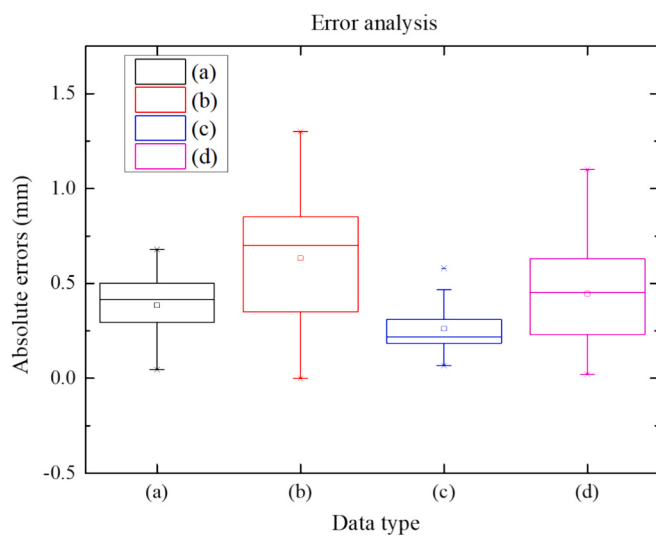


**Fig. 11.** Box-plot of the accuracy of the assembly point position estimation for the precast column and connected rebars model.

**Table 2**  
Comparison results with existing advanced methods.

Methods	Evaluation metrics	Extraction of rebar's center point		Extraction of sleeve's center point	
		Rebar diameter	Adjacent rebar spacing	Sleeve diameter	Adjacent sleeve spacing
Point cloud processing method [11]	Mean error (mm)	0.38	0.56	0.26	0.45
	Standard deviation (mm)	0.21	0.41	0.15	0.35
	Time (s)	0.221		1.516	
Image processing method [2]	Mean error (mm)	0.39	0.58	0.28	0.47
	Standard deviation (mm)	0.19	0.35	0.14	0.31
	Time (s)	0.175		0.201	
Point cloud-image fusion processing method (our method)	Mean error (mm)	0.32	0.53	0.22	0.43
	Standard deviation (mm)	0.17	0.31	0.14	0.29
	Time (s)	0.407		1.660	

estimating positions.

The mean value and 95 % confidence interval (CI) for the accuracy of the assembly point position estimation for the precast column and connected rebars model are presented in Table 1. The CI can be calculated as follows:

$$CI_{95\%} = \bar{x} \pm z_{\alpha/2} \frac{s}{\sqrt{n}} \quad (12)$$

where  $\bar{x}$  is mean value,  $z_{\alpha/2}$  is bilateral critical values of the standard normal distribution (e.g. 95 % confidence level corresponds to  $z_{\alpha/2} = 0.96$ ),  $s$  is standard deviation,  $n$  is the number of samples ( $n = 12$ ).

Fig. 11 presents box plots for four types of errors: (a), (b), (c), and (d), with median absolute errors of 0.42 mm, 0.55 mm, 0.22 mm, and 0.45 mm, respectively. The proposed method provides accurate geometric parameters estimates. Compared to the estimation accuracy of the rebar dimensions and positions, the estimation accuracy for the sleeves is higher due to the lower noise in the sleeve scan data.

To evaluate the performance of the proposed point cloud–image fusion processing method, comparative experiments were conducted against two existing approaches: the point cloud processing method [11] and the image processing method [2]. Table 2 shows the detection results of the three methods for 12 sets of rebars and sleeves.

The proposed fusion method consistently outperforms the two single-modality approaches in accuracy. For rebar diameter extraction, the mean error decreases to 0.32 mm, compared to 0.38 mm (point cloud processing method) [11] and 0.39 mm (image processing method) [2]. Similarly, for rebar and sleeve spacing, the fusion method achieves the lowest errors (0.53 mm and 0.43 mm) due to its superior noise resistance over point cloud processing. Corresponding standard deviations are also lower, indicating greater measurement stability.

The image processing method has the shortest runtime due to its computational simplicity but yields higher errors than the proposed approach. The proposed method takes longer (0.407 s for rebar features, 1.660 s for sleeve features) yet remains practical for real-time construction. Its improved accuracy justifies the slight increase in processing time, making it better suited for precision-critical assembly tasks.

Finally, from an economic perspective, all methods were tested using the same hardware—a structured light camera instead of costly laser scanners. This ensures a fair comparison and demonstrates the proposed method's practicality, achieving millimeter-level precision without expensive sensors.

Therefore, the proposed method achieves higher detection accuracy and robustness without significantly increasing processing time. This improvement results can be attributed to the conversion of the projected 2D point cloud into a binarized image for feature extraction. Performing circle detection in the image, as opposed to directly processing noisy point clouds, enhances detection accuracy and robustness.

## (2) Assembly point position checking.

The EOPA algorithm is employed to align the as-built model of the connected rebars or sleeves top surface with the as-designed model, offering intuitive guidance for adjusting the assembly section dimensions of the PC component. This step is particularly useful for verifying the connected rebar on construction sites, where misalignment of rebars often occurs due to collisions at construction sites. Traditional methods, including existing automatic measurement techniques, only measure actual dimensions and do not check assembly point deviations against the design model. As shown in Fig. 12, the deviation between the as-built position of the precast column bottom sleeve assembly point and the as-designed position is within the 2 mm error tolerance [29] required by standards. Similarly, Fig. 13 shows that the deviation for the connected rebar assembly point also falls within this error tolerance. Both deviations are within the acceptable range, allowing the next step to be the VTA of the precast column and the connected rebar.

### 3.2.2. Validation results of the VTA of the sleeves with the connected rebars

The EOPA algorithm is employed to align connected rebars with sleeves for the as-built model, providing a more intuitive estimation for the pre-assembly alignment and collision detection of precast components. Fig. 14 (a) visualizes horizontal deviations between assembly points to identify potential collisions, which occur if the deviation exceeds the difference between the sleeve's inner diameter and the rebar's diameter. Most collisions stem from the excessive deviation in rebar or sleeve positions from the as-designed model or the inclination of rebars. Fig. 14 (b) shows the distance between the centers of 12 sleeves and their corresponding connected rebars after assembly in the PC column, with a maximum distance of 2.39 mm, an average distance of 1.23 mm, and a standard deviation of 0.53 mm. Since the maximum distance between the sleeve center and the rebar center in the pre-assembly alignment is less than the maximum tolerance of 3 mm [1], the precast component can be successfully aligned and assembled within the specified tolerance of 3 mm.

To validate the accuracy of the predicted values from the VTA method, two model plates were fabricated to replicate the bottom

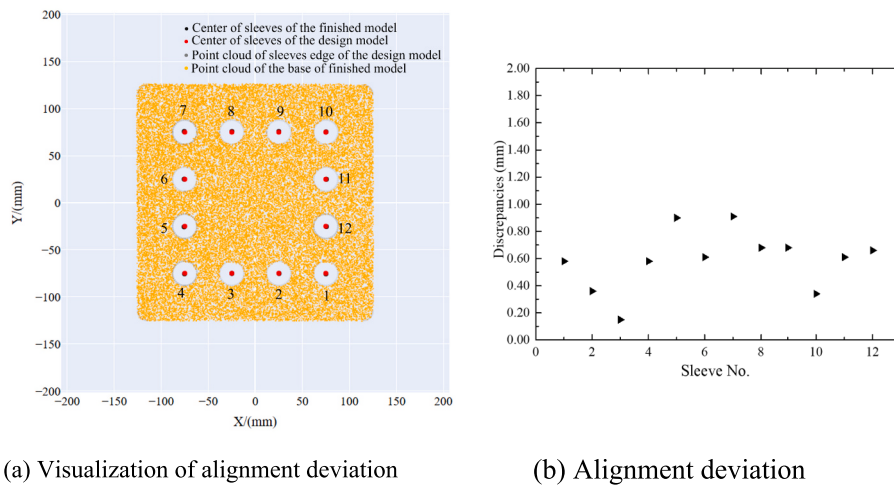


**Fig. 12.** Alignment deviation between the as-built position and the as-designed assembly points position of the sleeves.

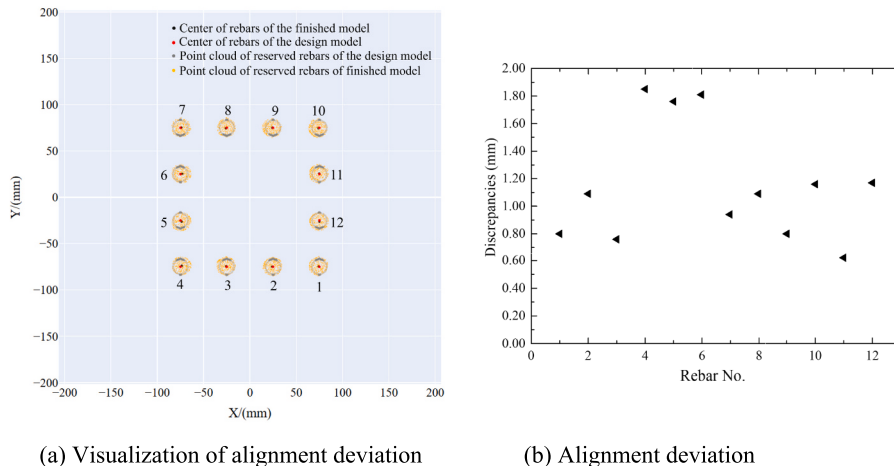


**Fig. 13.** Alignment deviation between the as-built position and the as-designed assembly points position of the connected rebars.

surface of the precast column model and the top surface dimensions of the reserved rebars at a 1:1 scale. These plates simulated the physical trial alignment of the precast column, ensuring that their centroids coincided without relative rotation. After alignment, the position deviations of the rebar and sleeve centers were measured using a vernier caliper, serving as the ground truth for comparison with the VTA method's predictions. Fig. 14(c) illustrates the physical trial assembly of the two model plates, with white dots representing sleeve centers and red dots representing rebar centers. The relative deviations between the two align closely with the VTA method's predicted results (see Fig. 14(a)). Further analysis of the alignment deviation statistics in Fig. 14(d) reveals a clear deviation trend. The alignment deviation between the sleeves and their corresponding connected rebars is within the allowable 3 mm tolerance specified by the standards, confirming that the sleeves can be aligned for assembly. This is consistent with the VTA method's predictions, with maximum, minimum, and average absolute deviations of 2.25 mm, 0.69 mm, and 1.28 mm, respectively, and a standard deviation of 0.53 mm.

In conclusion, the proposed method effectively predicts the alignment deviations between the rebar and the sleeve. For components prone to alignment issues during assembly, the VTA method can identify the optimal rebar position before shipping, allowing for recalibration or replacement of the precast column and significantly reducing rework due to misalignment.

### 3.3. Experimental results of precast column assembly alignment deviation measurements

This section evaluates the proposed alignment deviation measurement method for precast column assembly. Tests assess its accuracy and robustness across various parameter settings. Section 3.3.1 details the experimental parameters, Section 3.3.2 examines their impact on results, and Section 3.3.3 compares the method with existing approaches to demonstrate its superiority.

#### 3.3.1. Parameter settings

The 3D-printed PC column and connected rebar models were used as experimental objects. The spatial configuration of the setup is shown in Fig. 15, and four key parameters were examined:

Camera distance is the distance from the structured-light camera to the first rebar diagonally. Relative height is the vertical distance from the bottom of the column to the top of the connected rebars. The angle is the included angle between the column's bottom surface diagonal and the connected rebars. Planar spacing is the horizontal distance between the diagonal plane of the precast column and the diagonal of rebars. The experiment precisely controlled the relative positioning of the column and rebars—relative height, angle, and planar spacing—using a robotic arm. A structured light camera was employed to capture point cloud data of the alignment control plane for each parameter setting. The point clouds were processed with a key assembly point extraction algorithm to

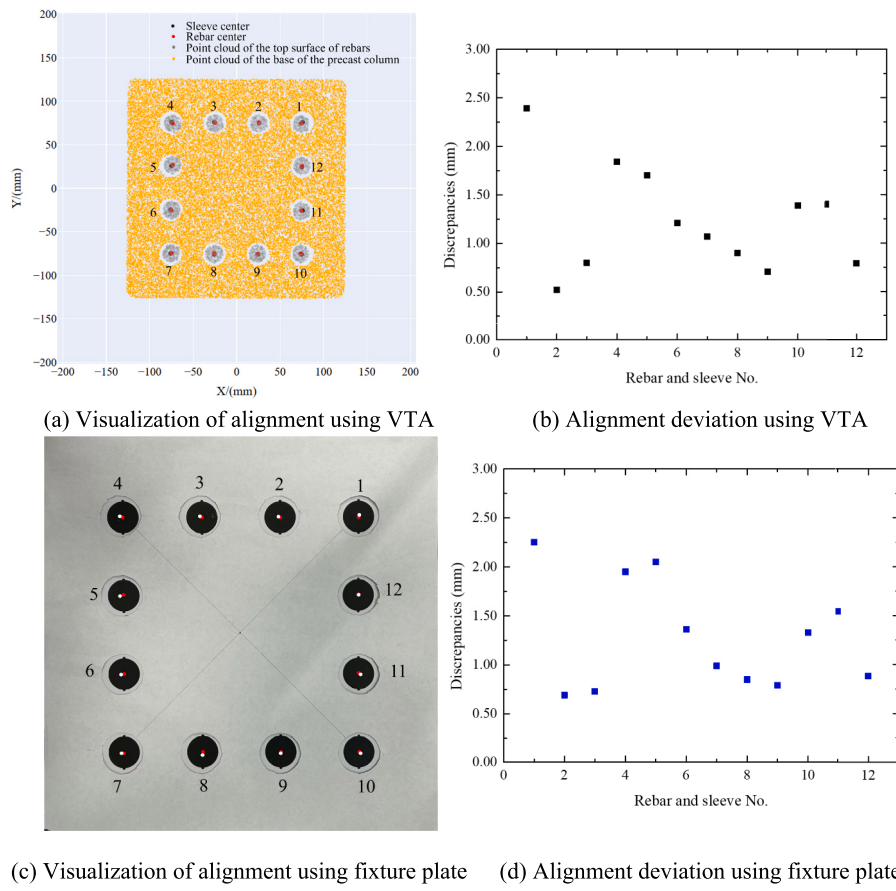


Fig. 14. Comparison of alignment deviation between VTA method and fixture plate.

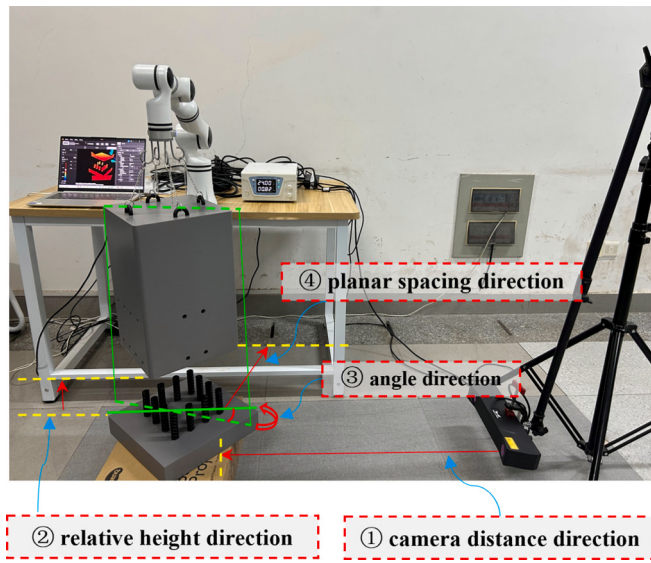


Fig. 15. Parameter settings related to alignment deviation measurement experiment.

obtain the 3D coordinates of the left, middle, and right sleeve centers on the column and their corresponding top-center positions on the rebars.

The column was vertically stable and had an approximately horizontal bottom surface. Horizontal deviation was calculated by projecting rebar key points onto the bottom surface of the column and measuring their distance from sleeve key points, as described in Section

### 2.2.3. Actual deviation was measured using a vernier caliper with a resolution of 0.02 mm.

Measurement performance was evaluated using two indicators: error, the absolute difference between computed and actual horizontal deviations; and average error, the mean error across the left, middle, and right key positions. This average error must meet the 3 mm alignment tolerance specified in the relevant construction standards [1].

### 3.3.2. Deviation measurements with different parameter settings

This subsection investigates how the camera distance and precast column positioning (including the relative height, angle, and plane spacing between precast columns and connected rebars) affect the proposed deviation measurement method.

#### (1) Influence of camera distance.

In real construction sites, precast columns and connected rebars are generally larger than the laboratory-scale models, requiring a greater camera distance for effective capture. This section investigates the effect of camera distance on deviation measurement accuracy. The camera was positioned at various distances to assess how this distance influences measurement precision. If the camera is too close to the target, the projected patterns tend to overlap, making it difficult to accurately resolve the position of each point; if the camera is too far from the target, the projected patterns become blurry, resulting in a reduction in the details that can be resolved and a decrease in point cloud density. Both scenarios negatively impact measurement accuracy. To ensure high-quality point clouds for the three connected rebars and their bottom sleeves, tests were conducted to identify optimal camera distances: 550, 650, 750, 850, 950, and 1050 mm. The relative height between the bottom of the precast column and the top of the rebars was set at 90 mm, ensuring that all control points were within the camera's optimal range. Table 3 shows the deviation measurement results for assembly

**Table 3**

Horizontal deviation measurement results of key assembly points for precast column and reserved rebars at different camera distances.

Camera distance (mm)	Key assembly points	Calculated deviation (mm)	Actual deviation (mm)	Error (mm)	Average error (mm)	Tolerance ( $\leq 3$ mm)
550	Left sleeve and rebar	2.33	0.94	1.39	1.32	Yes
	Middle sleeve and rebar	2.10	0.92	1.18		
	Right sleeve and rebar	2.48	1.10	1.38		
650	Left sleeve and rebar	2.52	0.94	1.58	1.54	Yes
	Middle sleeve and rebar	2.31	0.92	1.39		
	Right sleeve and rebar	2.76	1.10	1.66		
750	Left sleeve and rebar	2.73	0.94	1.79	1.74	Yes
	Middle sleeve and rebar	2.52	0.92	1.60		
	Right sleeve and rebar	2.94	1.10	1.84		
850	Left sleeve and rebar	2.99	0.94	2.05	1.92	Yes
	Middle sleeve and rebar	2.62	0.92	1.70		
	Right sleeve and rebar	3.11	1.10	2.01		
950	Left sleeve and rebar	3.44	0.94	2.50	2.40	Yes
	Middle sleeve and rebar	3.10	0.92	2.18		
	Right sleeve and rebar	3.63	1.10	2.53		
1050	Left sleeve and rebar	4.01	0.94	3.07	2.90	Yes
	Middle sleeve and rebar	3.62	0.92	2.70		
	Right sleeve and rebar	4.04	1.10	2.94		

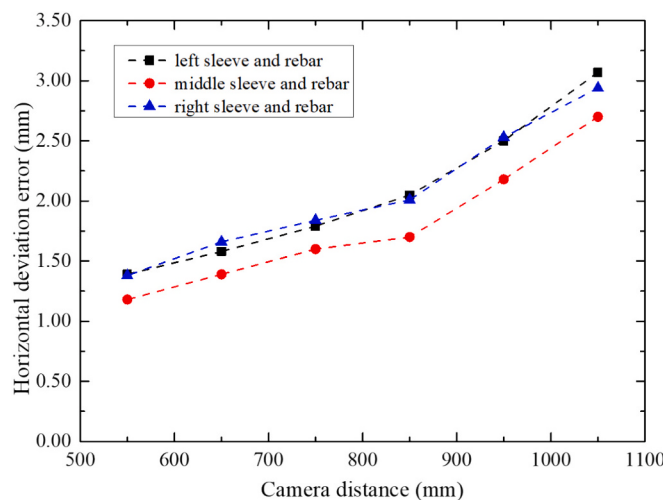


Fig. 16. Relationship between horizontal deviation error and camera distance of the proposed method.

alignment. At a shooting distance of 1050 mm, the horizontal deviation measurement error at the key assembly points was 2.90 mm, which is below the model's allowable alignment error of 3.0 mm.

The results presented in Fig. 16 indicate that the horizontal deviation

error gradually decreases as the camera distance increases from 550 mm to 850 mm. Beyond 850 mm, however, the measurement accuracy deteriorates significantly due to reduced point cloud density and increased noise levels. Therefore, a camera distance in the range of 550–850 mm is identified as the optimal working distance for the proposed deviation measurement method.

### (2) Influence of relative height.

To explore the effect of relative height between the precast column's bottom and the connected rebars on deviation measurement accuracy, relative heights of 90, 120, 150, 180, and 210 mm were tested, with a constant camera distance of 850 mm. The structured light camera fails to capture all critical assembly points when the height is below 90 mm or at least 210 mm. Under other unchanged conditions, point cloud images of the precast column and the connected rebars were collected at different relative heights, and the proposed deviation measurement method was employed to calculate the horizontal deviation between the critical assembly points of the sleeve and the rebars. The results are shown in Table 4. The results indicate that within the relative height range of 90 mm to 210 mm, the average horizontal deviation error increases slightly as the relative height increases. However, the precast column model can still be aligned using the robotic arm. Fig. 17 shows the relationship between the horizontal deviation errors at the left, middle, and right sleeves of the precast column and the corresponding rebar assembly points and relative height. It can be seen that as the relative height increases, the horizontal deviation errors show a slightly increasing trend.

### (3) Influence of angle.

**Table 4**

Horizontal deviation measurement results of key assembly points for precast column and connected rebars at different relative heights.

Relative height (mm)	Key assembly points	Calculated deviation (mm)	Actual deviation (mm)	Error (mm)	Average error (mm)	Tolerance ( $\leq 3$ mm)
90	Left sleeve and rebar	2.99	0.94	2.05	1.92	Yes
	Middle sleeve and rebar	2.62	0.92	1.70		
	Right sleeve and rebar	3.11	1.10	2.01		
120	Left sleeve and rebar	3.13	1.12	2.01	1.93	Yes
	Middle sleeve and rebar	2.78	1.00	1.78		
	Right sleeve and rebar	3.11	1.10	2.01		
150	Left sleeve and rebar	3.12	1.16	1.96	1.94	Yes
	Middle sleeve and rebar	2.80	1.06	1.74		
	Right sleeve and rebar	3.23	1.10	2.13		
180	Left sleeve and rebar	3.20	1.10	2.10	2.03	Yes
	Middle sleeve and rebar	2.79	1.02	1.77		
	Right sleeve and rebar	3.33	1.10	2.23		
210	Left sleeve and rebar	3.32	1.10	2.22	—	No
	Middle sleeve and rebar	—	1.00	—		
	Right sleeve and rebar	3.34	1.12	2.22		

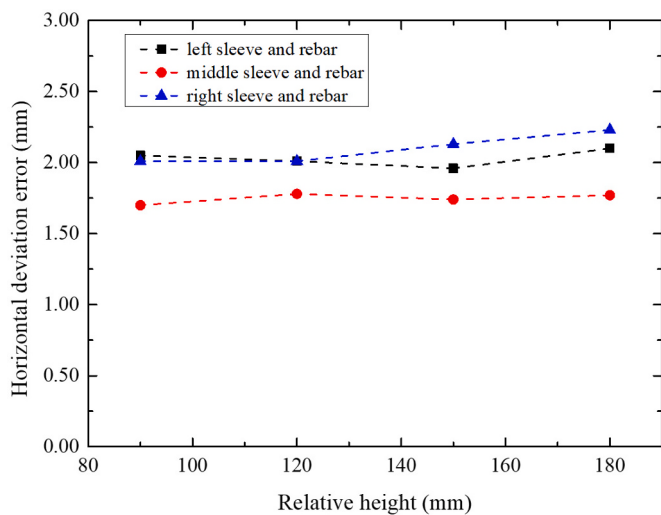


**Fig. 17.** Relationship between horizontal deviation error and relative height of the proposed method.

Prior to lifting and alignment, the diagonal of the precast column bottom sleeves is typically not parallel to the diagonal of the connected rebars, resulting in an angle between them. During the alignment process, the precast column is usually rotated to adjust its horizontal position, ensuring the alignment between the sleeve and the rebars. In this section, the relative height of the precast column is fixed at 180 mm, and the angles between the diagonal of the bottom sleeve and the connected rebars are set at 0°, 10°, 20°, 30°, and 40°, respectively, to investigate the effect of the angle on deviation measurement accuracy. Table 5 shows that at a 40° angle, the right sleeve exceeds the camera's field of view, making it impossible to obtain the center coordinates and preventing the measurement of its deviation from the center of the right connected rebar. As a result, the robotic arm cannot calculate the movement distance between the column and the model. Fig. 18 illustrates that within the 0° to 30° angle range, the measurement error of horizontal deviation between the left sleeve and the left connected rebar decreases slightly with increasing angle, while the measurement errors for the middle and right sleeves with their respective rebars a slight increase. Overall, the angle has a minimal impact on the accuracy of assembly alignment deviation measurements.

#### (4) Influence of planar spacing

Prior to lifting and alignment, there is an angle between the precast column's bottom sleeve diagonal and the connected rebars, as well as a horizontal spacing defined as the planar distance between the precast column's bottom surface and the rebars' top surface. This section

examines how varying planar distances affect the accuracy of the assembly alignment deviation measurements method. The relative height of the precast column is fixed at 180 mm, the angle is set at 30°, and the planar distances are set to 20, 40, 60, 80, and 100 mm, with the corresponding deviation measurement results shown in Table 6. The results show that as the planar distance increases, the average measurement error slightly increases. Fig. 19 presents the relationship between the horizontal deviation measurement errors of the left, middle, and right key assembly points of the precast column and the connected rebars, as well as the planar distance. It is observed that as the planar distance increases, the measurement errors for the middle and right key points slightly increase, while the error for the left key point slightly decreases. Overall, the influence of planar distance on the measurement of assembly alignment deviation is minimal, but the measurement accuracy gradually declines, as the target moves farther from the camera.

The experimental results suggest that the optimal camera positioning for accurate deviation measurement can be summarized as follows: (1) Camera Distance: In the camera distance range of 550–850 mm, the measurement error is less significantly affected by distance. (2) Relative Height: Heights of 90–180 mm capture critical features while keeping errors acceptable. (3) Angle: Angles up to 30° between the precast column's sleeve and rebars prevent occlusion and ensure visibility. (4) Planar Spacing: A spacing of 20–100 mm minimizes errors caused by increased distance from the sensor, ensuring the measurement remains

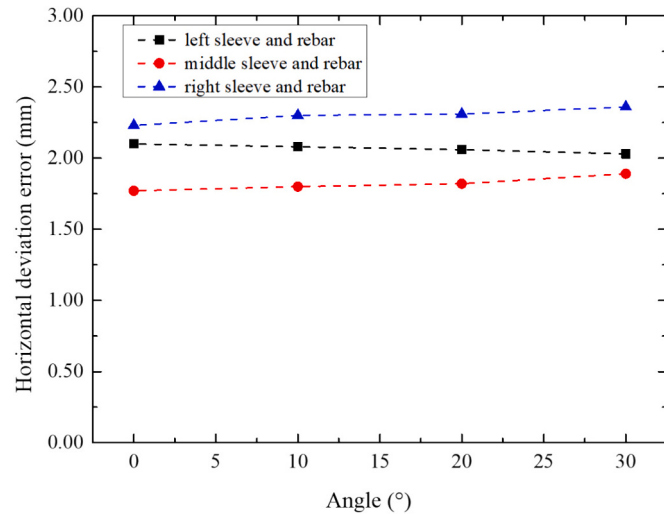


**Fig. 18.** Relationship between horizontal deviation measurement error and angle of the proposed method.

**Table 5**

Horizontal deviation measurement results of key assembly points for precast column and connected rebars at different angles.

Angle (°)	Key assembly points	Calculated deviation (mm)	Actual deviation (mm)	Error (mm)	Average error (mm)	Tolerance ( $\leq 3$ mm)
0	Left sleeve and rebar	3.20	1.10	2.10	2.03	Yes
	Middle sleeve and rebar	2.79	1.02	1.77		
	Right sleeve and rebar	3.33	1.10	2.23		
10	Left sleeve and rebar	20.72	18.64	2.08	2.06	Yes
	Middle sleeve and rebar	20.48	18.68	1.80		
	Right sleeve and rebar	20.80	18.50	2.30		
20	Left sleeve and rebar	39.20	37.14	2.06	2.06	Yes
	Middle sleeve and rebar	39.02	37.20	1.82		
	Right sleeve and rebar	39.31	37.00	2.31		
30	Left sleeve and rebar	57.33	55.30	2.03	2.09	Yes
	Middle sleeve and rebar	56.91	55.02	1.89		
	Right sleeve and rebar	57.42	55.06	2.36		
40	Left sleeve and rebar	74.87	72.88	1.99	—	No
	Middle sleeve and rebar	74.53	72.58	1.95		
	Right sleeve and rebar	—	72.52	—		

**Table 6**

Horizontal deviation measurement results of key assembly points for precast column and connected rebars at different planar spacings.

Plane spacing (mm)	Key assembly points	Calculated deviation (mm)	Actual deviation (mm)	Error (mm)	Average error (mm)	Tolerance ( $\leq 3$ mm)
0	Left sleeve and rebar	57.33	55.30	2.03	2.09	Yes
	Middle sleeve and rebar	56.91	55.02	1.89		
	Right sleeve and rebar	57.42	55.06	2.36		
	Left sleeve and rebar	66.30	64.28	2.02		
20	Middle sleeve and rebar	77.38	75.48	1.90	2.11	Yes
	Right sleeve and rebar	57.02	54.62	2.40		
	Left sleeve and rebar	79.30	77.32	1.98		
40	Middle sleeve and rebar	96.96	94.98	1.98	2.15	Yes
	Right sleeve and rebar	62.54	60.04	2.50		
	Left sleeve and rebar	94.2	92.26	1.94		
60	Middle sleeve and rebar	117.14	115.06	2.08	2.19	Yes
	Right sleeve and rebar	73.58	71.04	2.54		
	Left sleeve and rebar	111.20	109.34	1.86		
80	Middle sleeve and rebar	137.32	135.16	2.16	2.21	Yes
	Right sleeve and rebar	88.14	85.54	2.60		
	Left sleeve and rebar	129.30	127.52	1.78		
100	Middle sleeve and rebar	157.30	155.04	2.26	2.23	Yes
	Right sleeve and rebar	104.72	102.06	2.66		

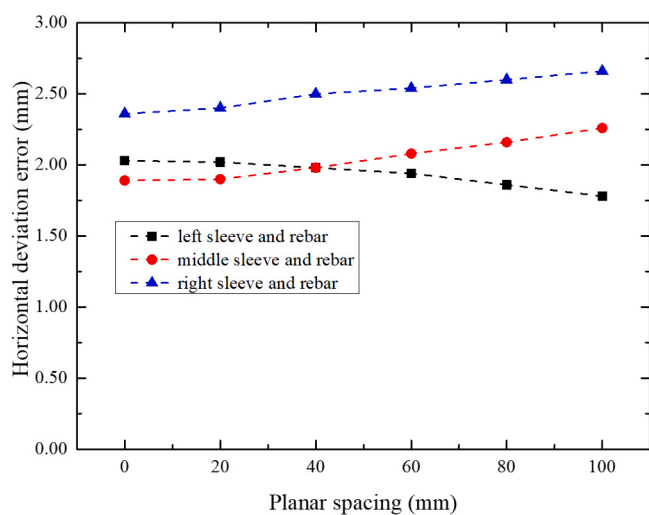


**Fig. 19.** Relationship between horizontal deviation error and plane spacing of the proposed method.

within the required accuracy threshold.

These parameters guide the positioning of cameras and components in automated PC column assembly, ensuring reliable point cloud quality and accurate deviation measurements.

### 3.3.3. Contrastive experiments with existing advanced methods

To assess the robustness and efficiency of the proposed method under different assembly conditions, a 3D-printed precast column and its corresponding reserved rebar model were used. A structured light camera was positioned 850 mm diagonally from the first rebar for optimal coverage (Fig. 15). Three experimental conditions were designed: (1) the column was suspended 180 mm above the rebars; (2) it was rotated 30° counterclockwise based on condition (1); and (3) a 100 mm planar spacing was added to condition (2). Point cloud data were collected under each condition and processed using the proposed key point extraction algorithm to determine the 3D coordinates of the left, middle, and right sleeve centers and rebar tops. Given the column's vertical orientation, its bottom surface was treated as a horizontal reference plane. The reserved rebar points were projected onto this plane, and the horizontal deviations were calculated as the Euclidean distance between corresponding projected points. Ground truth deviations were measured using a vernier caliper with 0.02 mm resolution.

Tables 7–9 compare the proposed point cloud–image fusion alignment method with representative point cloud-based (Zhao's [11]) and image-based (Ye's [2]) methods under three conditions. Our method achieves the lowest average errors at six key assembly points—2.03 mm, 2.09 mm, and 2.23 mm—reducing errors by about 20 % compared to the point cloud method (2.44, 2.70, 2.81 mm) and about 35 % compared to the image method (3.13, 3.22, 3.38 mm). Error ranges for our method are tight (1.77–2.66 mm), showing greater robustness to variations in height, angle, and planar spacing (see Fig. 20); the image method has outliers up to 3.99 mm (Table 9). Our method's processing time (0.585, 0.603, 0.650 s) were about 20 % slower than the point cloud method

**Table 7**

Contrastive results of horizontal deviation at key assembly points between sleeves and rebars under condition of the relative height (180 mm).

Methods	Evaluation metrics	Key assembly points					
		Left sleeve	Left rebar	Middle sleeve	Middle rebar	Right sleeve	Right rebar
Vernier caliper	Actual deviation (mm)	1.10		1.02		1.10	
	Calculated deviation (mm)	3.55		3.30		3.70	
Zhao's method [11]	Measured error (mm)	2.45		2.28		2.60	
	Average error (mm)			2.44			
Ye's method [2]	Time (s)			0.464			
	Calculated deviation (mm)	4.20		3.98		4.43	
Our method	Measured error (mm)	3.10		2.96		3.33	
	Average error (mm)			3.13			
	Time (s)			0.241			
	Calculated deviation (mm)	3.20		2.79		2.10	
	Measured error (mm)	2.10		1.77		2.23	
	Average error (mm)			2.03			
	Time (s)			0.585			

**Table 8**

Contrastive results of horizontal deviation at key assembly points between sleeves and rebars under conditions of the relative height (180 mm) and angle (30°).

Methods	Evaluation metrics	Key assembly points					
		Left sleeve	Left rebar	Middle sleeve	Middle rebar	Right sleeve	Right rebar
Vernier caliper	Actual deviation (mm)	55.30		55.02		55.06	
	Calculated deviation (mm)	57.93		57.60		57.95	
	Measured error (mm)	2.63		2.58		2.89	
Zhao's method [11]	Average error (mm)			2.70			
	Time (s)			0.489			
	Calculated deviation (mm)	58.50		57.98		58.56	
Ye's method [2]	Measured error (mm)	3.20		2.96		3.50	
	Average error (mm)			3.22			
	Time (s)			0.323			
Our method	Calculated deviation (mm)	57.33		56.91		57.42	
	Measured error (mm)	2.03		1.89		2.36	
	Average error (mm)			2.09			
	Time (s)			0.603			

**Table 9**

Contrastive results of horizontal deviation at key assembly points between sleeves and rebars under conditions of the relative height (180 mm), angle (30°) and planar spacing (100 mm).

Methods	Evaluation metrics	Key assembly points					
		Left sleeve	Left rebar	Middle sleeve	Middle rebar	Right sleeve	Right rebar
Vernier caliper	Actual deviation (mm)	127.52		155.04		102.06	
	Calculated deviation (mm)	130.08		158.15		104.82	
	Measured error (mm)	2.56		3.11		2.76	
Zhao's method [11]	Average error (mm)			2.81			
	Time (s)			0.522			
	Calculated deviation (mm)	130.02		158.34		106.05	
Ye's method [2]	Measured error (mm)	2.85		3.30		3.99	
	Average error (mm)			3.38			
	Time (s)			0.346			
Our method	Calculated deviation (mm)	129.30		157.30		104.72	
	Measured error (mm)	1.78		2.26		2.66	
	Average error (mm)			2.23			
	Time (s)			0.650			

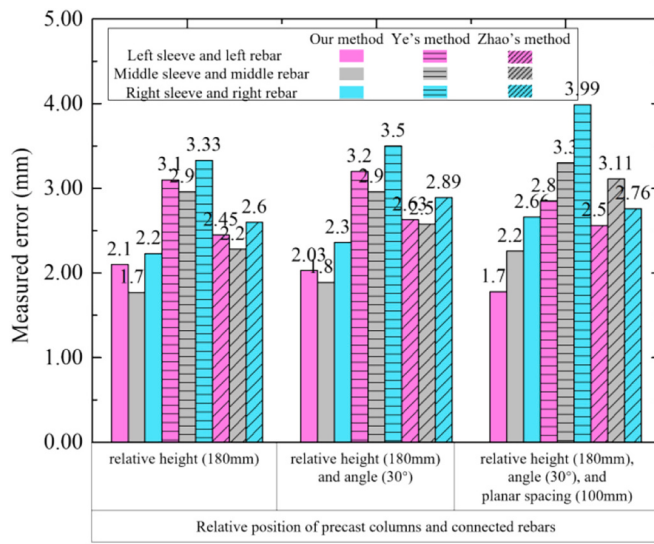


**Fig. 20.** Comparison of measured errors between our method and advanced methods under different relative positions of precast columns and connected rebars.

(0.464, 0.489, 0.522 s) and about 50 % slower than the image method (0.241, 0.323, 0.346 s) (see Fig. 21). Although our method incurs an acceptable loss in processing time while achieving improved accuracy, it remains close to real-time. The image method is fastest but often exceeds the  $\pm 3$  mm tolerance due to unreliable cylinder axis estimation from a

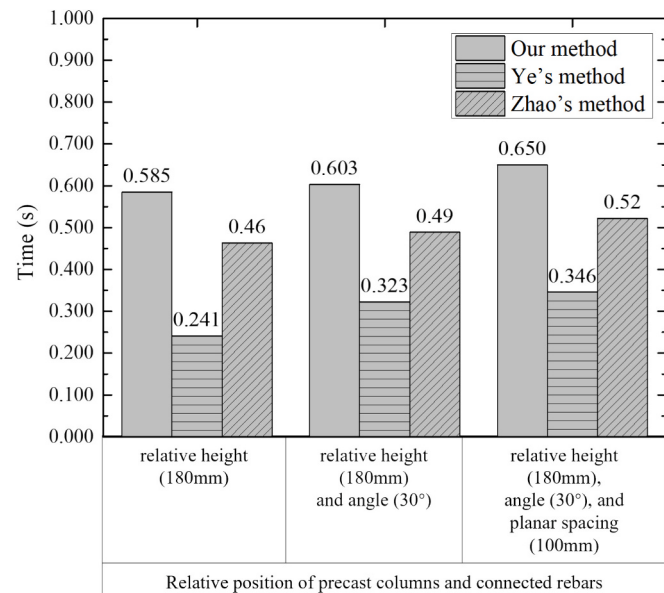


**Fig. 21.** Comparison of processing times between our method and existing advanced methods under different relative positions of precast columns and connected rebars.

single 2D view, affected by perspective distortion, occlusion, and blurred edges. The point cloud method detects 3D circular features but is more sensitive to noise and outliers, reducing accuracy. By integrating

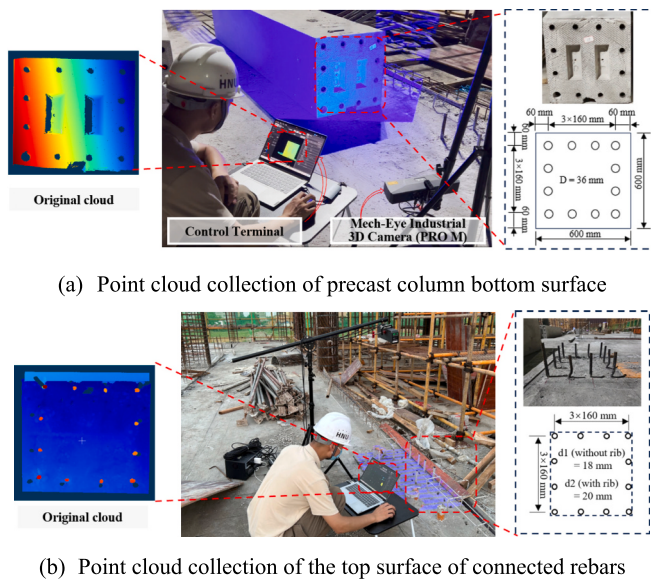


**Fig. 22.** Point cloud collection of PC column assembly sections at construction sites.

3D point clouds with binarized images, our method uses point cloud constraints to correct spatial inaccuracies inherent in 2D fitting, while circle fitting on binarized images reduces noise impact. This approach achieves optimal accuracy, robustness, and efficiency without costly LiDAR technology, consistently meeting the  $\pm 3$  mm tolerance across all tested conditions.

#### 4. Field test

To validate the applicability of the proposed assembly alignment deviation measurement method in practical engineering, experiments were conducted at a precast construction site. The tests were carried out at the construction site of a newly built middle school in Yiyang, Hunan Province, with the test subject being a portion of vertical components of a teaching building in the project. The experiments are divided into two parts: (1) VTA of PC columns before alignment and (2) Alignment deviation measurement in PC columns during the alignment process.

#### 4.1. VTA of PC columns

Before the VTA, the point cloud of the assembly cross-section of the PC column (i.e., the bottom surface of the column and the top surface of the connected rebars) should first be collected. The proposed method was then employed to detect the assembly points' positions and verified their accuracy. As shown in Fig. 22, the structured light camera (Mech-Eye PRO M) was employed to capture the initial point clouds of both the bottom surface of the column and the top surface of the connected rebars. The design dimensions of the assembly cross-section are shown on the right of Fig. 22, with an inner sleeve diameter of 36 mm, a connected rebar diameter of 20 mm with rib, and a 160 mm distance between adjacent centerlines. The construction standard [29] allows a deviation of 2 mm between the centerlines of adjacent sleeves or connected rebars. The specific parameters of the structured light camera are shown in Fig. 9 (b).

The initial point clouds of the assembly cross-section of on-site PC column and connected rebars were collected and processed using the proposed method to extract assembly points and calculate the diameters and center distances of the sleeves or the connected rebars, as shown in Fig. 23. The accuracy of this method was evaluated by comparing the results with manual tape measurements. The precast column model employed in the test has 12 sleeves on the bottom surface, corresponding to 12 connected rebars. Therefore, 24 distances ( $12 \times 2$ ) between adjacent rebars and sleeves and 24 radii of the rebar tops and sleeve openings were calculated and compared. Fig. 24 (a), (b), (c), and (d) show the absolute errors between the measured and estimated values for the radius of the connected rebars, the center distances between the rebars, the radius of the sleeves, and the center distances of the sleeves, respectively. In Fig. 24 (a), the mean absolute error is 0.65 mm, with a root mean square error (RMSE) of 0.71 mm; in Fig. 24 (b), the mean absolute error is 0.75 mm, with an RMSE of 0.83 mm; in Fig. 24 (c), the mean absolute error is 0.49 mm, with an RMSE of 0.62 mm; in Fig. 24 (d), the mean absolute error is 0.73 mm, with an RMSE of 0.81 mm. Since the average absolute error and RMSE between the calculated center distances and the manual measurements are both less than the 2 mm tolerance allowed for the sleeves and connected rebars, the proposed method can accurately estimate the positions of the rebars and sleeves.

The mean value and 95 % confidence interval (CI) for the accuracy of the assembly point position estimation for the on-site PC column and

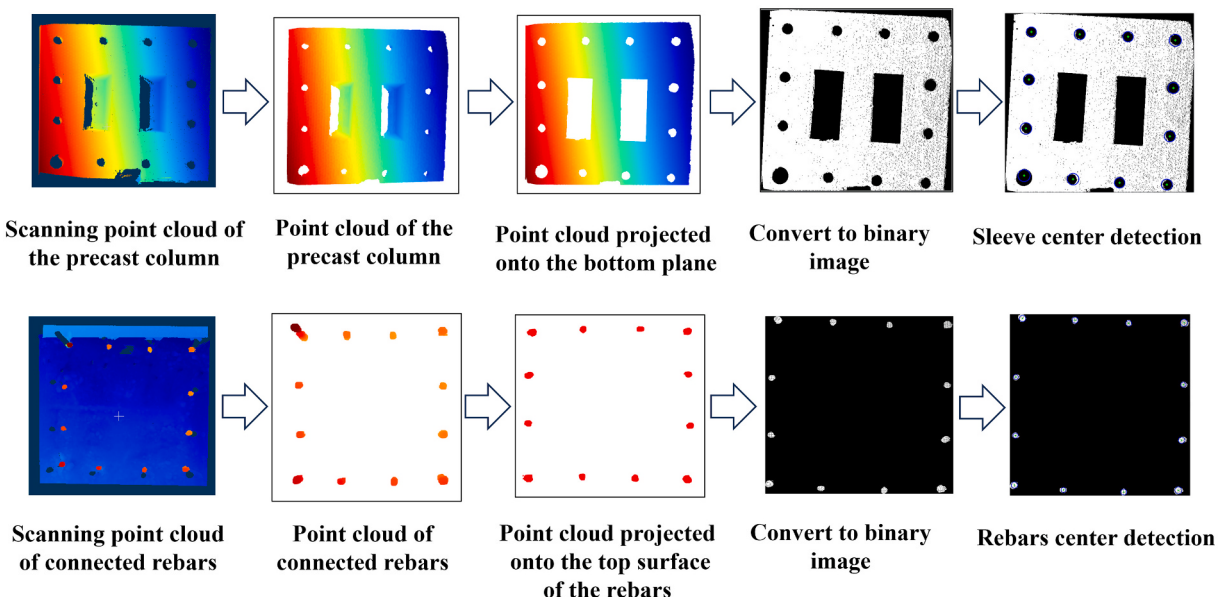


**Fig. 23.** Assembly feature point extraction of the on-site PC column and connected rebars.

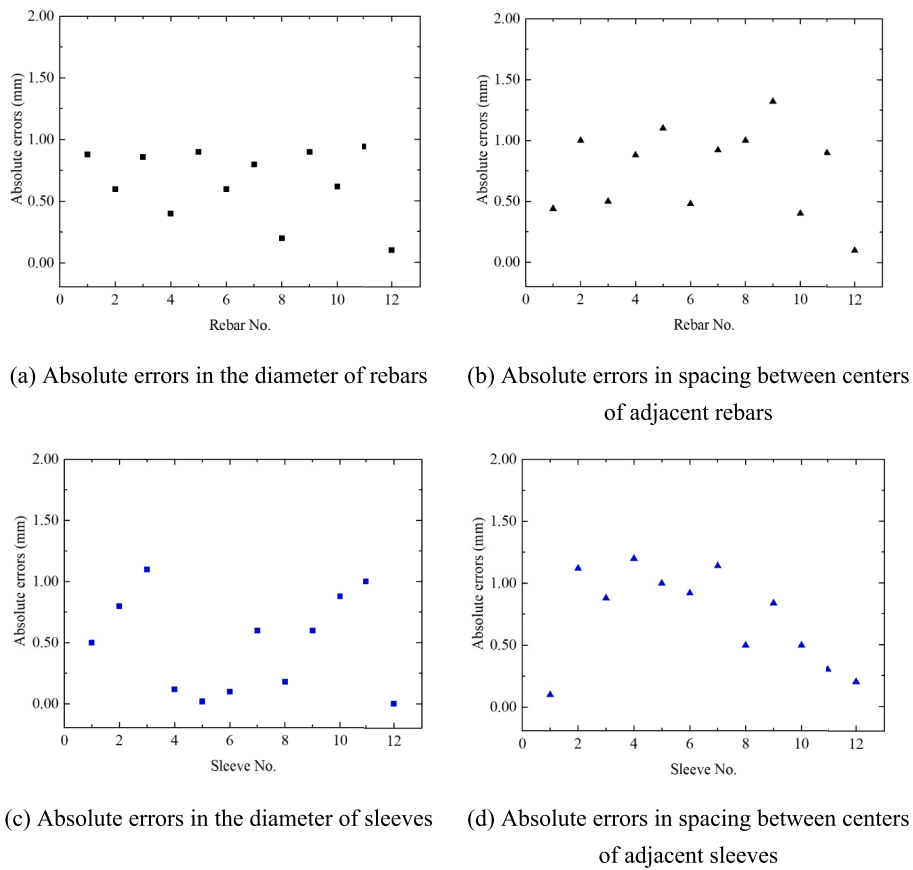


**Fig. 24.** Scatter chart of the accuracy of the assembly point position estimation for the on-site PC column and connected rebars.

**Table 10**

The mean and confidence interval (CI) of the accuracy of the assembly point position estimation for the on-site PC column and connected rebars.

	Mean value (mm)	Standard deviation (mm)	CI (mm)
Rebar diameter	0.65	0.27	(0.49, 0.81)
Adjacent rebar spacing	0.83	0.75	(0.56, 0.95)
Sleeve diameter	0.49	0.38	(0.27, 0.71)
Adjacent sleeve spacing	0.73	0.37	(0.52, 0.93)

connected rebars are presented in [Table 10](#). The CI can be calculated as follows:

[Fig. 25](#) shows box plots for four types of errors, where the median absolute errors for (a), (b), (c), and (d) are 0.71 mm, 0.89 mm, 0.55 mm, and 0.86 mm, respectively. Overall, the proposed method provides sufficiently accurate estimates of geometric parameters. Compared to the estimation accuracy for rebar size and position, the accuracy for the sleeves is higher, which can be attributed to the lower noise in the scan data of the sleeves.

[Table 11](#) summarizes the performance of three methods applied to real precast concrete components. The proposed point cloud–image fusion approach outperforms others in accuracy and stability. For rebar features, it achieves mean errors of 0.65 mm (diameter) and 0.83 mm (spacing), lower than the point cloud method [11] (0.71 mm and 1.05 mm) and image processing method [2] (0.82 mm and 1.12 mm). Similarly, for sleeve features, the fusion method reduces errors to 0.49 mm (diameter) and 0.73 mm (spacing), demonstrating robustness in practical conditions. Smaller standard deviations further indicate improved measurement stability.

The image processing method offers the fastest runtime (<0.5 s) due to its computational simplicity but sacrifices accuracy. In contrast, the

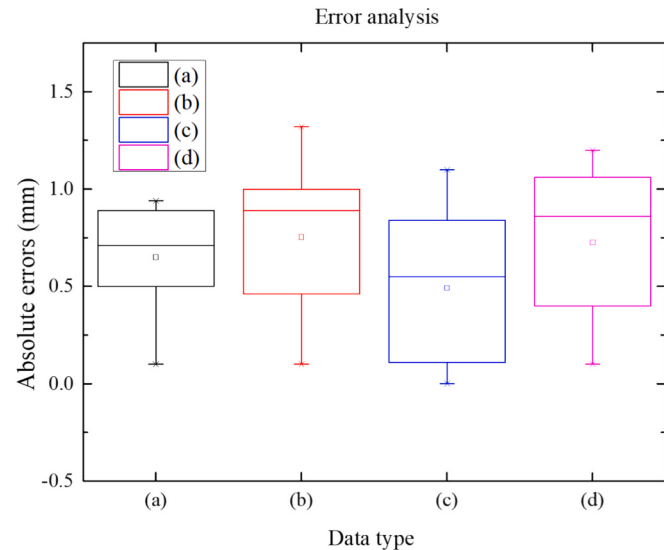


**Fig. 25.** Box-plot of the accuracy of the assembly point position estimation for the on-site PC column and connected rebars.

fusion method's higher accuracy justifies its slightly longer, yet still acceptable, computational time for real-world on-site assembly.

Experimental results confirm that the proposed point cloud–image fusion method achieves the optimal balance of precision, robustness, and efficiency, ensuring reliable automated alignment deviation measurement in real construction settings.

To validate the accuracy of the assembly point positions of the PC

**Table 11**  
Comparison results with existing advanced methods.

Methods	evaluation metrics	Extraction of rebar's center point		Extraction of sleeve's center point	
		Rebar diameter	Adjacent rebar spacing	Sleeve diameter	Adjacent sleeve spacing
Point cloud processing method [11]	Mean error (mm)	0.71	1.05	0.52	0.94
	Standard deviation (mm)	0.52	0.92	0.40	0.63
Image processing method [2]	Time (s)	0.610		3.430	
	Mean error (mm)	0.82	1.12	0.59	1.13
Point cloud-image fusion processing method (our method)	Standard deviation (mm)	0.69	1.05	0.48	0.78
	Time (s)	0.445		0.463	
Point cloud processing method [11]	Mean error (mm)	0.65	0.83	0.49	0.73
	Standard deviation (mm)	0.27	0.75	0.38	0.37
(our method)	Time (s)	0.850		3.780	

columns, the EOPA method was employed to align the assembly points of the sleeves and connected rebars in the as-built assembly cross-section model with those in the as-designed model, as shown in Fig. 26 and Fig. 27. The alignment deviations are clearly evident in the figures, with significant discrepancies between the two models. Specifically, the center deviation of sleeve number 1 is 7.41 mm in Fig. 26 (b), and the center deviation of sleeve number 2 is 12.87 mm in Fig. 27 (b), both of which exceed the 2 mm tolerance allowed by the standards. Therefore, the component should be replaced or corrected.

Fig. 28 shows the deviations between the centers of the 12 sleeves and the connected rebars after aligning the PC column. The maximum deviation is 13.93 mm, the average deviation is 8.34 mm, and the standard deviation is 4.16 mm. As the maximum deviation exceeds the allowable 3 mm [1] error for model assembly, the precast component cannot achieve automatic alignment and requires manual correction.

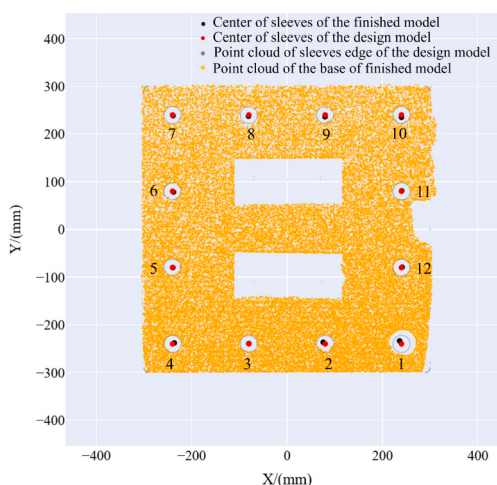
#### 4.2. Alignment deviation measurement in PC column

To validate the feasibility of the proposed alignment deviation measurement method during the alignment process at the construction site, a deviation measurement test was conducted after correcting assembly point positions. Point cloud data was first collected for the assembly control plane during the alignment process. Based on the dimensions of the lifting components, camera field of view, and on-site installation conditions, a structured light camera was deployed along the extension of the diagonal line of the connected rebar, 720 mm away from the first rebar, as shown in Fig. 29. The proposed alignment deviation measurement method, using three non-collinear key assembly points, was then applied to process the point cloud data collected during on-site PC column assembly alignment process, with detailed steps outlined in Fig. 30. After processing the raw point cloud data, the three-dimensional coordinates of the key assembly points of the precast column and the corresponding connected rebar were obtained. Subsequently, the 3D coordinates of the rebar key assembly points were projected onto the plane of the precast column's base, and the horizontal deviations between them were calculated. According to the deviation measurement results in Table 12, the average error between the sleeve key assembly points of the precast column and the rebar key assembly points was found to be 1.39 mm, which is below the allowable assembly error of 3 mm. This confirms compliance with standards, allowing operators to lower components, insert rebar, and complete alignment without repeated adjustments.

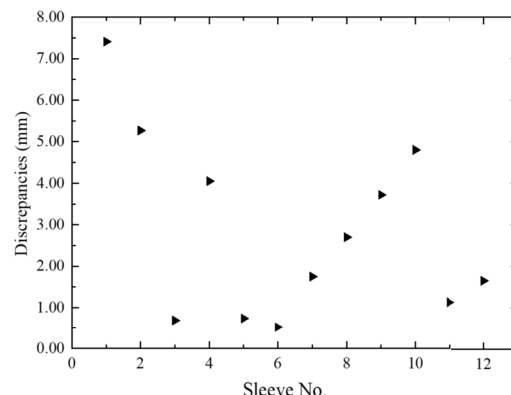
In comparison, Ye et al.'s image-based method [2] shows an average error of 3.33 mm (Table 12), exceeding the 3 mm tolerance, while Zhao et al.'s point-cloud method [11] stays within tolerance but was less accurate (2.42 mm average error). The proposed method offers greater accuracy (1.39 mm average error) and reliability in measuring on-site assembly alignment deviations. Although the image method is fastest (0.250 s), it sacrifices accuracy. The proposed method (0.622 s) is about 18 % lower than the point-cloud method (0.510 s) and operates near real-time. Therefore, the proposed method balances accuracy and efficiency without costly laser scanners.

## 5. Conclusions

This paper presented an automated alignment deviation measurement (AADM) method for the assembly of precast concrete (PC) columns connected via grouting sleeves, integrating a Virtual Trial Assembly

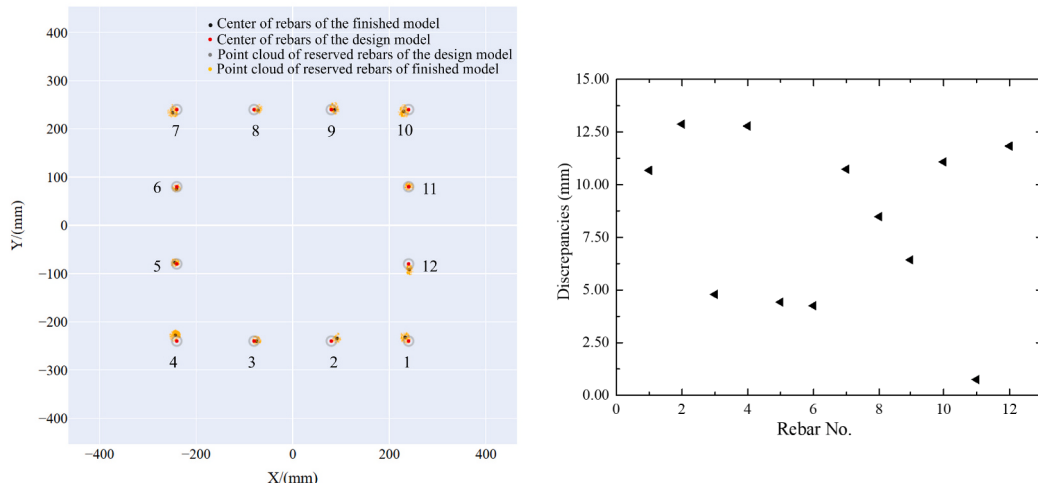


(a) Visualization of alignment deviation



(b) Alignment deviation

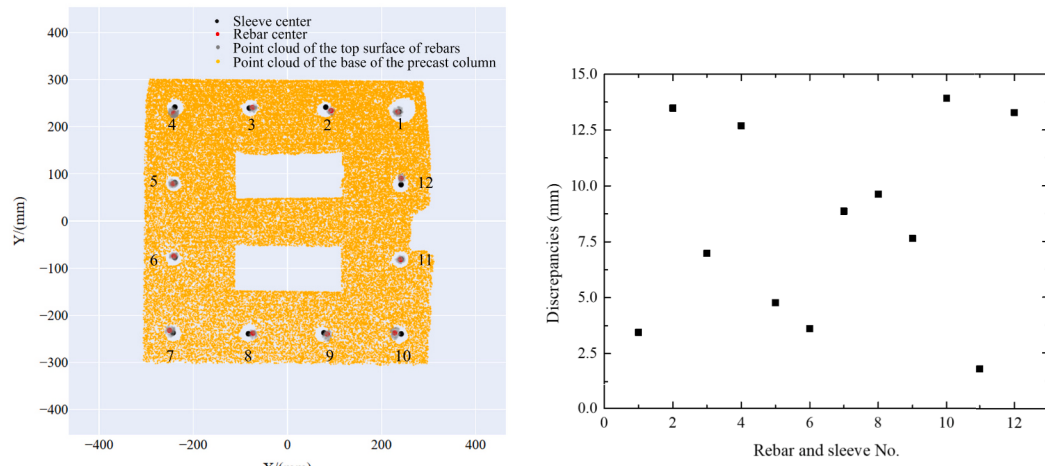
**Fig. 26.** Alignment deviation between the as-built position and the as-designed position of the sleeves' assembly point.



(a) Visualization of alignment deviation

(b) Alignment deviation

Fig. 27. Alignment deviation between the as-built position and the as-designed position of the rebars' assembly point.



(a) Visualization of alignment deviation

(b) Alignment deviation

Fig. 28. Alignment deviation between the bottom sleeves of the PC column and the connected rebars.

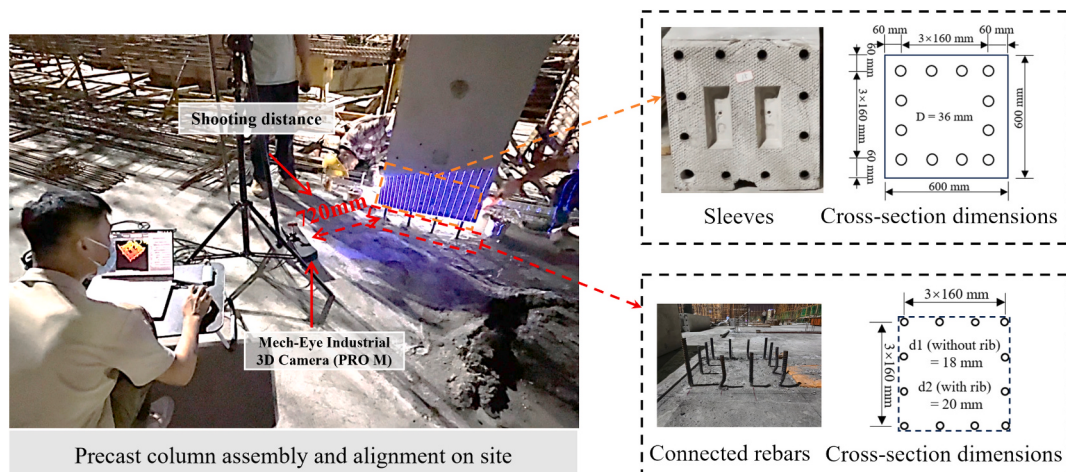
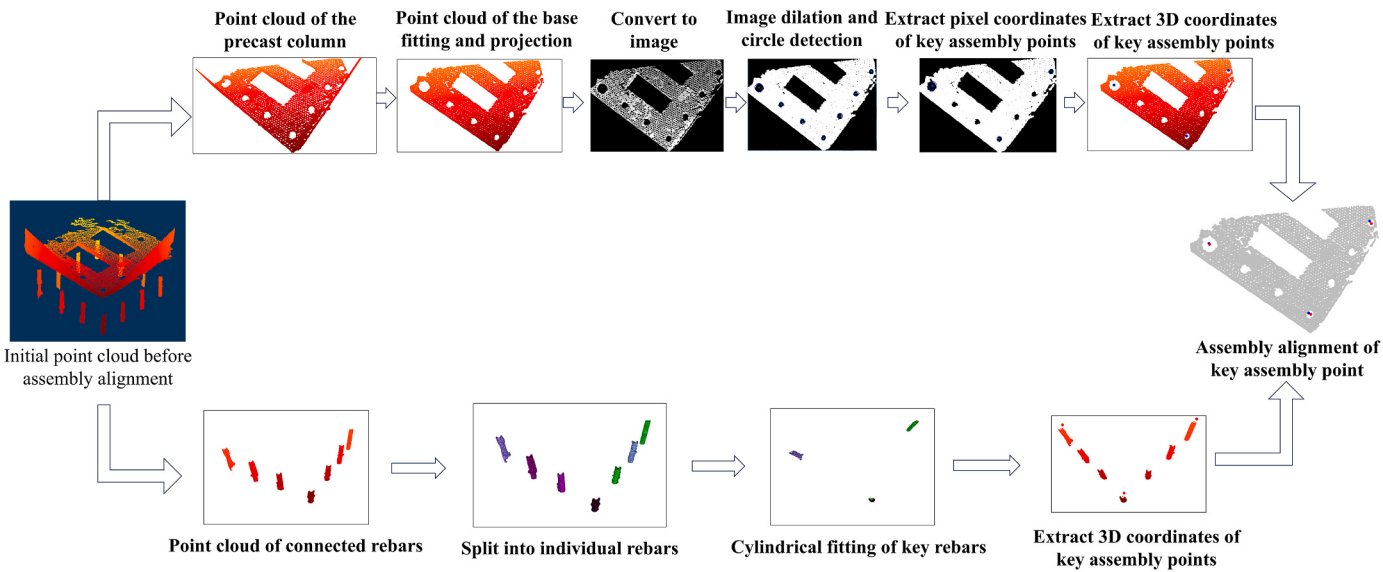


Fig. 29. Point cloud collection of assembly control surfaces during the alignment process of PC columns at the construction site.



**Fig. 30.** Specific steps of the Alignment Deviation Measurement (ADM) module for on-site PC column assembly alignment.

**Table 12**

Horizontal deviation measurement results of key assembly points for on-site precast column sleeve-rebar alignment.

Methods	Evaluation metrics	Key assembly points					
		Left sleeve	Left rebar	Middle sleeve	Middle rebar	Right sleeve	Right rebar
Vernier caliper Zhao's method [11]	Actual deviation (mm)	3.10		3.20		4.50	
	Calculated deviation (mm)	5.37		5.57		7.12	
	Measured error (mm)	2.27		2.37		2.62	
	Average error (mm)	2.42					
	Time (s)	0.510					
Ye's method [2]	Calculated deviation (mm)	5.70		6.20		8.90	
	Measured error (mm)	2.60		3.00		4.40	
	Average error (mm)	3.33					
	Time (s)	0.250					
Our method	Calculated deviation (mm)	4.14		4.22		6.62	
	Measured error (mm)	1.04		1.02		2.12	
	Average error (mm)	1.39					
	Time (s)	0.622					

(VTA) module and an Alignment Deviation Measurement (ADM) module. The VTA module extracts assembly points and enables accurate pre-hoisting assemblability evaluation. The ADM module uses three non-collinear key assembly points to automatically assess alignment deviations. The proposed AADM method was validated through model experiments and field tests. The assembly point extraction method's accuracy was verified through cross-section dimension measurements. The feasibility of the VTA module was assessed using VTA experiments on 3D printed PC column and tests on PC columns at construction sites. In order to verify the feasibility of the ADM module, ADM experiments on 3D printed PC column and on-site PC column compared with vernier caliper measurements were conducted.

The key contributions and findings are as follows:

(1) The VTA module can provide accurate assembly point extraction in the pre-hoisting stage. Model experiments and field tests showed that estimated errors in sleeve diameter, rebar diameter, and center distances between adjacent sleeves and rebars are within 1 mm, confirming the accuracy of the proposed assembly point extraction method.

(2) The VTA module using the sleeve and the rebar centers as assembly points allows a good assessment of the assemblability of PC columns. Model experiment results showed that the alignment deviations between the as-built and as-designed models were within the 2 mm tolerance. Furthermore, VTA based on the selected feature points quantified the alignment deviation between the column and connected rebars, yielding an average absolute deviation of 1.23 mm and a

standard deviation of 0.53 mm.

(3) The ADM module identify optimal camera and component positioning parameters for reliable point cloud quality and accurate deviation measurement in automated PC column assembly. A camera distance of 550–850 mm, a relative height of 90–180 mm, an angle within 30°, and a planar spacing of 20–100 mm between the column and rebars ensure visibility of key assembly points while keeping measurement errors within a 3 mm tolerance. These guidelines offer practical references for on-site automated PC column assembly.

(4) The reliability of ADM module was verified by Field tests. Experimental results showed an average alignment deviation of 1.39 mm with camera distance of 720 mm using the proposed method, well below the 3 mm maximum allowable limit, confirming the reliability of ADM module.

(5) The proposed AADM method addresses both pre-hoisting assemblability evaluation and in-hoisting positioning measurement, providing a technical reference for PC columns to achieve high-precision automated assembly within 3 mm tolerance constraints.

This paper has several limitations: First, the field tests used precast columns with a cross-section of 600 mm × 600 mm, which may not represent larger actual column dimensions, leaving the applicability of the proposed method to larger components unverified. Second, the study primarily focuses on deviation measurement during the alignment process and does not consider integrating these measurements with lifting machinery for automated assembly alignment at the construction

site. Third, while the proposed method emphasizes local alignment accuracy for single-column installation, it does not quantitatively analyze the potential propagation of misalignments (rotations and translations) to adjacent structural elements, such as beams or slabs. These accumulated deviations could affect the overall geometric consistency of the assembled structure. Future research will aim to model and evaluate the global impact of local pose deviations, and develop integrated correction strategies that account for multi-component assembly interactions in real construction scenarios. Fourth, the three-point ADM strategy may be susceptible to local misalignment caused by uncontrollable assembly errors or non-rigid deformations that violate the rigid-body assumption. Future research will explore how to adjust the component's pose to create an optimal correction scheme for misalignment of rebars and sleeves due to uncontrollable assembly errors during hoisting. These limitations highlight areas for future research to enhance the method's robustness and practical applicability.

### CRediT authorship contribution statement

**Lizhi Long:** Writing – original draft, Methodology, Conceptualization. **Wenyao Liu:** Writing – review & editing, Supervision. **Shaopeng Xu:** Validation, Software. **Peng Shi:** Validation, Software. **Cheng Zhang:** Validation, Investigation. **Lu Deng:** Writing – review & editing, Supervision, Funding acquisition.

### Declaration of competing interest

The authors declare that they have no known competing financial interests or personal relationships that could have appeared to influence the work reported in this paper.

### Data availability

Data will be made available on request.

### Acknowledgments

The authors would like to acknowledge the financial support provided by the National Key Research and Development Program of China (Grant No.2023YFC3806800), the National Natural Science Foundation of China (Grant No. 52278177), the Hunan Province funding for leading scientific and technological innovation talents (Grant No. 2021RC4025), the Postgraduate Scientific Research Innovation Project of Hunan Province (Grant No. CX20240430), the Central Guidance for Local Science and Technology Development Fund Project (Grant No. 246Z5404G).

### References

- [1] Ministry of Housing and Urban-Rural Development of the People's Republic of China, Technical standard for assembled buildings with concrete structure. [https://www.mohurd.gov.cn/gongkai/fdzdgknr/tzgg/201703/20170302\\_231205.html](https://www.mohurd.gov.cn/gongkai/fdzdgknr/tzgg/201703/20170302_231205.html).
- [2] X. Ye, Y. Zhou, H. Guo, Z. Luo, A computer vision-based approach to automatically extracting the aligning information of precast structural components, Autom. Constr. 164 (2024) 105478, <https://doi.org/10.1016/j.autcon.2024.105478>.
- [3] Y. Zhao, C. Cao, Z. Liu, A framework for prefabricated component hoisting management systems based on digital twin technology, Buildings 12 (2022) 276, <https://doi.org/10.3390/buildings12030276>.
- [4] Y. Jiang, J. Shu, J. Ye, W. Zhao, Virtual trial assembly of prefabricated structures based on point cloud and BIM, Autom. Constr. 155 (2023) 105049, <https://doi.org/10.1016/j.autcon.2023.105049>.
- [5] Z. Ma, Y. Liu, J. Li, Review on automated quality inspection of precast concrete components, Autom. Constr. 150 (2023) 104828, <https://doi.org/10.1016/j.autcon.2023.104828>.
- [6] Q. Wang, J.C.P. Cheng, H. Sohn, Automated estimation of reinforced precast concrete rebar positions using colored laser scan data, Comput. Aided Civ. Inf. Eng. 32 (2017) 787–802, <https://doi.org/10.1111/mice.12293>.
- [7] M.-K. Kim, J.P.P. Thedja, H.-L. Chi, D.-E. Lee, Automated rebar diameter classification using point cloud data based machine learning, Autom. Constr. 122 (2021) 103476, <https://doi.org/10.1016/j.autcon.2020.103476>.
- [8] Q. Wang, M.-K. Kim, J.C.P. Cheng, H. Sohn, Automated quality assessment of precast concrete elements with geometry irregularities using terrestrial laser scanning, Autom. Constr. 68 (2016) 170–182, <https://doi.org/10.1016/j.autcon.2016.03.014>.
- [9] J. Shu, W. Li, C. Zhang, Y. Gao, Y. Xiang, L. Ma, Point cloud-based dimensional quality assessment of precast concrete components using deep learning, Journal of Building Engineering 70 (2023) 106391, <https://doi.org/10.1016/j.jobe.2023.106391>.
- [10] F. Li, M.-K. Kim, Mirror-aided registration-free geometric quality inspection of planar-type prefabricated elements using terrestrial laser scanning, Autom. Constr. 121 (2021) 103442, <https://doi.org/10.1016/j.autcon.2020.103442>.
- [11] W. Zhao, Y. Jiang, Y. Liu, J. Shu, Automated recognition and measurement based on three-dimensional point clouds to connect precast concrete components, Autom. Constr. 133 (2022) 104000, <https://doi.org/10.1016/j.autcon.2021.104000>.
- [12] D. Wang, L. Gao, J. Zheng, J. Xi, J. Zhong, Automated recognition and rebar dimensional assessment of prefabricated bridge components from low-cost 3D laser scanner, Measurement 242 (2025) 115765, <https://doi.org/10.1016/j.measurement.2024.115765>.
- [13] F. Case, A. Beinat, F. Crosilla, I.M. Alba, Virtual trial assembly of a complex steel structure by generalized Procrustes analysis techniques, Autom. Constr. 37 (2014) 155–165, <https://doi.org/10.1016/j.autcon.2013.10.013>.
- [14] E. Maset, L. Scalera, D. Zonta, I.M. Alba, F. Crosilla, A. Fusielo, Procrustes analysis for the virtual trial assembly of large-size elements, Robot. Comput. Integrat. Manuf. 62 (2020) 101885, <https://doi.org/10.1016/j.rcim.2019.101885>.
- [15] Y.-G. Wang, X.-J. He, J. He, C. Fan, Virtual trial assembly of steel structure based on BIM platform, Autom. Constr. 141 (2022) 104395, <https://doi.org/10.1016/j.autcon.2022.104395>.
- [16] J. Liu, N. Cui, G. Cheng, D. Li, X. Ma, Y. Liao, Towards the automated virtual trial assembly of large and complex steel members using terrestrial laser scanning and BIM, Eng. Struct. 291 (2023) 116448, <https://doi.org/10.1016/j.engstruct.2023.116448>.
- [17] M.-K. Kim, H. Sohn, C.-C. Chang, Automated dimensional quality assessment of precast concrete panels using terrestrial laser scanning, Autom. Constr. 45 (2014) 163–177, <https://doi.org/10.1016/j.autcon.2014.05.015>.
- [18] M.-K. Kim, Q. Wang, J.-W. Park, J.C.P. Cheng, H. Sohn, C.-C. Chang, Automated dimensional quality assurance of full-scale precast concrete elements using laser scanning and BIM, Autom. Constr. 72 (2016) 102–114, <https://doi.org/10.1016/j.autcon.2016.08.035>.
- [19] D. Kim, Y. Kwak, H. Sohn, Accelerated cable-stayed bridge construction using terrestrial laser scanning, Autom. Constr. 117 (2020) 103269, <https://doi.org/10.1016/j.autcon.2020.103269>.
- [20] S. Yoon, Q. Wang, H. Sohn, Optimal placement of precast bridge deck slabs with respect to precast girders using 3D laser scanning, Autom. Constr. 86 (2018) 81–98.
- [21] Y. Xu, Y. Luo, J. Zhang, Laser-scan based pose monitoring for guiding erection of precast concrete bridge piers, Autom. Constr. 140 (2022) 104347, <https://doi.org/10.1016/j.autcon.2022.104347>.
- [22] S.W. Park, H.S. Park, J.H. Kim, H. Adeli, 3D displacement measurement model for health monitoring of structures using a motion capture system, Measurement 59 (2015) 352–362, <https://doi.org/10.1016/j.measurement.2014.09.063>.
- [23] S. Choi, W. Myeong, Y. Jeong, H. Myung, Vision-based hybrid 6-DOF displacement estimation for precast concrete member assembly, Smart Struct. Syst. 20 (2017) 397–413.
- [24] B. Shan, S. Zheng, J. Ou, Free vibration monitoring experiment of a stayed-cable model based on stereovision, Measurement 76 (2015) 228–239.
- [25] Y. Cheng, F. Lin, W. Wang, J. Zhang, Vision-based trajectory monitoring for assembly alignment of precast concrete bridge components, Autom. Constr. 140 (2022) 104350, <https://doi.org/10.1016/j.autcon.2022.104350>.
- [26] K. Zhang, S. Tong, H. Shi, Trajectory prediction of assembly alignment of columnar precast concrete members with deep learning, Symmetry (Basel) 11 (2019) 629, <https://doi.org/10.3390/sym11050629>.
- [27] H. Yuen, J. Princen, J. Illingworth, J. Kittler, Comparative study of Hough transform methods for circle finding, Image Vis. Comput. 8 (1990) 71–77, [https://doi.org/10.1016/0262-8856\(90\)90059-E](https://doi.org/10.1016/0262-8856(90)90059-E).
- [28] M.A. Fischler, R.C. Bolles, Random sample consensus, Commun. ACM 24 (1981) 381–395, <https://doi.org/10.1145/358669.358692>.
- [29] Ministry of Housing and Urban-Rural Development of the People's Republic of China, Standard for tolerances for precast concrete components. <https://book118.com/html/2022/0913/5334201023004340.shtml>.
- [30] Z. Zhang, D. Liang, H. Huang, L. Sun, Virtual trial assembly of large steel members with bolted connections based on multiscale point cloud fusion, Comput. Aided Civ. Inf. Eng. 39 (2024) 2619–2641, <https://doi.org/10.1111/mice.13210>.
- [31] A. Fusielo, F. Crosilla, Solving bundle block adjustment by generalized anisotropic Procrustes analysis, ISPRS J. Photogramm. Remote Sens. 102 (2015) 209–221, <https://doi.org/10.1016/j.isprsjprs.2015.02.002>.
- [32] F.L. Bookstein, Size and shape spaces for landmark data in two dimensions, Stat. Sci. 1 (1986), <https://doi.org/10.1214/ss/1177013696>.
- [33] F. Crosilla, A. Beinat, A. Fusielo, E. Maset, D. Visintini, Advanced procrustes analysis models in photogrammetric computer vision, Springer International Publishing, Cham (2019), <https://doi.org/10.1007/978-3-030-11760-3>.
- [34] K.A.M. Said, A.B. Jambek, Analysis of image processing using morphological erosion and dilation, J. Phys. Conf. Ser. 2071 (2021) 012033, <https://doi.org/10.1088/1742-6596/2071/1/012033>.
- [35] D. Deng, DBSCAN clustering algorithm based on density, in: 2020 7th international forum on electrical engineering and automation (IFEEA), IEEE, 2020, pp. 949–953, <https://doi.org/10.1109/IFEEA51475.2020.00199>.